

AUTHOR'S RESPONSE

David L. Adams and Andrea Zampiron

This document contains the replies to all comments provided by the reviewers for this paper, indications of corrections or changes to the revised manuscript, as well as a marked up version of the document containing all changes made to the text and structure of the original paper. We would like to thank the reviewers for their time and comments, as we believe they have contributed greatly to improving the quality of this paper. The following sections are separated by reviewer, and then by comment type.

Reviewer 1 responses and changes

General comments

We would like to thank the reviewer for highlighting three aspects of the manuscript that required major modifications or additions. First, there were several areas where the presentation and interpretation of the TRC analysis was unclear, which stimulated us to modify the expression and provide a more clear and comprehensive explanation. Second, the description of the experimental methods provided was insufficient and detracted from the findings, which has compelled us to provide additional detail and importantly, a quantification of error. Third, upon recommendation, we calculated k_s values from the hydraulic data using a Colebrook-White type equation, which allowed us to demonstrate that the roughness correlation provides fairly accurate estimates of the total k_s (within a factor-of-two).

Reviewer: [There are] some serious questions regarding the accuracy of the experimental data which needs to be discussed in much more depth given the small scale of the experiments (see also my comment regarding the surface tension). This, together with the influence of the inlet and outlet sections indicates that more work is required to substantiate the results of the study.

Author: We would like to briefly respond to this comment, before a more in-depth response below. In the absence of error estimates provided in the initial submission, the reviewer has raised a reasonable doubt as to whether the dataset is of sufficient quality. From a practical standpoint, the small-scale of the model is necessary to fully replicate in-channel morphology in gravel-bed rivers, notably, bars, pools, and riffles. The superposition of both grain (small) and form-scale (large) resistance elements provides an optimal dataset for the demonstration of the TRC approach. However, the trade-off is an inevitable decrease in the degree of precision of the model, notably, the measurement of hydraulic quantities (due to shallow water depths and surface tension). As we demonstrate with a brief analysis of measurement error for the stream gauges (included within the revised manuscript), this does not compromise the results of the study. Based on the degree of measurement precision (1 mm), there is on average a plus-minus 8 percent error in estimates of flow depths. Also, the importance of edge-effects within the experiments have been over-stated, and we demonstrate with an analysis that they have little-to-no effect on the wavelet transform, nor do they affect the roughness length analysis.

Reviewer: For example, the authors need to expand their consideration towards the heterogeneity of the surface (and not only a single profile). In fact, focusing solely on the thalweg profile means that some morphological features such as banks, etc. are not adequately captured through the analysis.

Author: We agree, complete three-dimensional decomposition of the roughness length in the channel would include information regarding the banks, overall channel gradient, vegetation, etc., however, this is beyond the scope of this paper. The proposed approach pertains to only in-channel features and provides a more detailed and theoretically robust analysis compared to other existing approaches in rivers (notably, grain size, standard deviation of elevations). We will clarify that the TRC approach, in its present form, is an analysis of fluid drag associated with in-channel features and that it does not consider other resistance elements, nor three-dimensional interactions between flow and channel topography. Also, as demonstrated in the specific comments, the good correlation between topographic (using the

roughness correlation) and hydraulic (using the Colebrook-White equation) validates the one-dimensional approach for the experiments used herein.

Reviewer: I also see the need to define the concept of determining k_s for different wavelengths from a hydraulic point of view in more detail taking the physics into account

Author: As discussed (L221-224), the disaggregation of flow resistance into different scales (flow superposition approach) has been a common conceptual and analytical approach since the 1950s, and the suggested approach in this study is merely an extension of this. Notable examples include (1) attempts to estimate the relative importance of grain and bedform resistance using statistics (L25-27, e.g. Weichert et al. 2009), and (2) the reverse, in which one may roughly estimate the total frictional resistance of a natural channel by noting the presence of specific resistance elements (e.g. Cowan 1956, Manning coefficients for natural channels). As discussed, Li (2009) and Wilcox and Wohl (2006) have emphasised that the combination of different roughness elements may lead to nonlinear drag feedbacks in either direction, however, the decomposition approach holds that roughness elements (e.g. a grain or a riffle) have relatively discrete and linearly additive hydraulic effects.

We are unable to provide an explanation beyond which has already provided in the literature; however, we have been able to demonstrate that the assumptions of the superposition approach hold, in two different ways. The first is comparing the estimates of k_s by applying roughness correlation with and without the wavelet transform, and the second is by comparing these estimates of k_s to the 'true' value of k_s , calculated using the Colebrook-White approach. We expand on these two points below.

Specific comments

Reviewer: L11: Having read the communication, I am not sure what conventional equation is meant by the authors.

Author: We were referring to a conventional flow resistance equation using relative submergence, which has been clarified.

Reviewer: L22: It is stated that the grains and bedforms on the surface span orders of magnitude of scales. So the question arises if the thalweg profile is really sufficient to capture all spatial scales? (see also L48)

Author: If in-channel features are of interest, a profile may capture the one-dimensional character of the roughness elements if it is sufficiently long. For example, in the dataset presented herein, the thalweg profile spans 5-6 pool-riffle pairs (the dominant resistance elements), which is sufficient to capture their characteristic geometry (height, spacing). As explained in L61-65, the required length of the profile would be dependent on the features of interest. We have clarified this in the manuscript.

Reviewer: L50: The reference for the used roughness correlation should be given here, as it was not really developed by the authors.

Author: We have provided the reference at this point.

Reviewer: L62: There are many morphological features that contribute to drag which are not considered when analyzing the thalweg profile (this includes the curvature of the channel, alternate bars and many more). This needs to be highlighted better.

Author: We agree, it is important to acknowledge that the analysis pertains to in-channel features only, as well as noting the potential importance of other roughness elements. We have discussed this in the general comments above and clarified this in the manuscript.

Reviewer: L64: It is stated that the spatial extent of the data should at least cover the largest features that produce significant drag (resistance). A dune is one such feature and it becomes not really clear why many dune crests need to be included in the dataset. This should be elaborated in some more depth. In this context, can the spatial extent of 3D-features really be described using a single profile?

Author: From the sampling perspective, it is ideal to have a spatial extent that spans multiple roughness elements of the same type (riffles, dunes, steps) to establish some characteristic geometry (notably, the height of roughness elements and their spacing or slope). This has been clarified in the text. As discussed, three-dimensional effects are outside the scope of this paper.

Reviewer: L66: The data meant by the authors should be specified, as I am not sure how data can be reduced to streamlines. A streamline is a line that follows the direction of flow velocity and is a hydraulic feature. So how exactly can topographic data be reduced to a streamline? Also, how can streamlines intersect when these lines follow the direction of flow? This should be specified.

Author: We agree. We will remove mention of intersecting streamlines and will replace the word 'streamline' with 'thalweg elevation profile'. We have clarified that the thalweg elevation profile is used due to its association with the dominant vector of flow velocity.

Reviewer: L70: I fully acknowledge that the authors use a wavelet approach. However, the principle of wavelets should be described in some more depth, as not all readers will be familiar with the principles of the wavelet transforms described here.

Author: We agree and have provided further explanation in the revised manuscript regarding the concepts relating to wavelet transform.

Reviewer: L76: Fig. 1 presents data from Experiment 1a - these data have not been described and no reference is found to an experimental study. This is confusing. For example, how does the reader know the shown profile originates from a riffle-bar sequence and that the MODWT is aligned with the thalweg elevation profile? In this context, why is the CWT not aligned with the thalweg-profile? It is also a wavelet transform that is based on the thalweg-profile - so it should be aligned with this profile? This could be formulated more clearly.

Author: A reference and note have been provided for the data that has been used. I believe the word 'aligned' may have caused some confusion and requires clarification. Both the MODWT and CWT analyses are performed on the same profile, but the CWT analysis yields a set of wavelengths that do not resemble the original signal. We have clarified this in the revised manuscript.

Reviewer: L84: I fully agree but would also argue that almost all gravel bed rivers are in the hydraulic rough regime. In this context, what is meant by the statement that roughness correlations have only been developed for limited ranges of Re^ ? Typically, three ranges are distinguished, and existing approaches can be found that cover all these ranges.*

Author: This may be a simple miscommunication - we intended to say that roughness correlations typically apply to a given regime of Re^* (i.e. discrete ranges), and thus, it is important to use the roughness correlation that matches the regime of the dataset. We have re-phrased this.

Reviewer: L85: I am not sure that the width to depth ratio is an appropriate measure to determine if the flow is 2D. For example, the flow in the roughness layer of gravel beds is far from being 2D. Note also 2D conditions also depend on the relative submergence (I acknowledge that this is mentioned in the next paragraph, but I would expect such a statement already here).

Author: In rough-bed flows, the flow is highly heterogeneous within the so-called roughness layer which extends for 2-5 roughness length scales within the flow depth (e.g., Nikora et al. 2001 Spatially averaged open-channel flow over rough bed) and it is homogeneous at higher elevations (e.g., Nezu and Nakagawa 1993 “Turbulence in open-channel flows”). A rough-bed flow is 2D far from the bed if the flow depth is large compared to the roughness length scale, in this case, the ratio channel width to flow depth is sufficient. For low submergence flows the situation is more complex and the answer is not trivial. Cameron et al. 2017 “Very-large-scale motions in rough-bed open-channel flow” observed that turbulence statistics in flows over a homogeneous rough bed preserve two-dimensional distributions for relative submergences as low as 2. We agree with the Reviewer that a large width to flow depth ratio is generally not sufficient to guarantee two-dimensional flow conditions for flows with flow depth comparable to the roughness length scale. We, therefore, acknowledge that our flows characterized by the lowest relative submergence may not be two-dimensional, and clarify that although width-depth ratio is an indicator of 2D flow, it does not guarantee it. This has been clarified.

Reviewer: L100: How was discharge measured? L101: How was sediment transport scaled?

Author: Discharge was set and monitored using a high-precision electronic pump, which would generally hold a flow rate to within pm 0.02 L/s (we do not have access to specifications at this moment due to COVID-19 lab closures). Sediment transport is not scaled within the model, and rather, it is determined by length and time-scaling. The experiment had a recirculating sediment supply, so that the sediment transport rate was determined by the system itself.

Reviewer: L104: What was the working principle of these gages and what was the distance between them? Investigating Table 2, I found that the water depths were very low (< 0.02 m). This means that surface tension can impose a significant scale effect biasing the results. This needs to be discussed. In this context, what was the accuracy of the water depth readings? I am asking because the differences in water depth are within the millimeter range.

Author: We agree that this could use some more clarification. We have explained that ten equally spaced gauges were used, and water depths were recorded to the nearest 1 mm. They were spaced every 1 m for all experiments except for the 8cm-wide experiments, where they were spaced every 80 cm due to the slightly shorter length of the flume, which has been detailed in the revised manuscript. With regards to surface tension, we have clarified that the water is dyed a rich blue colour, and the water-surface gauges were viewed almost side-on, meaning that surface tension effects could be identified and disregarded, and therefore systematic bias towards higher readings was minimised.

Based on an analysis of measurement error using the 1 mm precision, now included in the text, errors of between plus-minus 6 and 11 percent could be expected for mean hydraulic depths (errors are variable due to different depths), with a median of plus-minus 7.6 percent. The magnitude of error is almost the same for the velocity estimates based on propagation of error from both the discharge and water-depth measurements. We estimate that the ratio U/U^* has a median error of plus-minus 11.5 percent, with a maximum of plus-minus 15 percent for the shallowest depths.

Reviewer: L111: How exactly can discharge be scaled with the width of the experimental channel when using a Froude-scale model? The information that bankfull discharge was used is enough, but it should be stated how deep the channel was. Also, is there information available how much discharge was conveyed through the sediment bed (this could be important given the low discharges)?

Author: The discharge was scaled to the width to maintain the same reach-averaged shear stress and the same initial relative submergence, however, this information may be unnecessary to provide within the context of this study. Due to the fixed banks, the channel has a depth that is dependent on the degree of scour/deposition and the discharge. There is no information regarding how much discharge was conveyed through the sediment bed. The grain size distribution is predominantly sand which reduces the potential for infiltration and subsurface flow. Also, before ramping up the flow to the target discharge, we monitored the water table within the stream bed (via a hole) to ensure that the bed was fully saturated. We have provided this explanation in the text.

Reviewer: L116: Which weirs? Was there a backwater effect?

Author: There are two weirs, one at the upstream and the downstream end, that hold the sediment within the stream table, but do not hold back the water (the initial bed is screeded to the height of these weirs). At the downstream end, where water free-falls over the weir, there is slight and localised lowering of the water surface due to a downdraw effect, but no discernable backwater. We have added this explanation to the methods.

Reviewer: L117: What was the corresponding flow rate? That would help to answer my question @L111?

Author: The low-flow was approximately 0.4 L/s for the 30cm channel, and 0.15 L/s for the 8cm channel. These values corresponded to the flows at which the bed could be wet and saturated without sediment transport. We have added a note to the text that channel-saturating flows were determined based on the movement of sediment.

*Reviewer: L118: Had the draining of the bed any effect on the topography and was the bed saturated again when increasing the discharge after the measurements? Table 2 lacks of units and $k^*_s, pred$ has not been defined properly (see below).*

Author: We have noted that the draining of the bed was rapid as the pump was simply turned off. During the initial 5-10 seconds of drainage, a small layer of sediment sourced from the riffle tails was transported into the pools, but there was no discernable change to the morphology. The bed was saturated again before increasing the discharge, as explained above. More clear units have been provided for these parameters. We have responded to comments regarding $k^*_s, pred$ below.

Reviewer: L121: Referring back to my comment @L104 - it is stated that the water surface elevation was determined to the nearest millimeter and that the mean water depths are lower than the maximum water depth (what is meant by the statement "most of the maximum flow depths"?), the degree of precision is different than stated @L122.

Author: We have revised this section based on the previous comments and added the analysis of error. Measurement precision is 1 mm.

Reviewer: L141: Figure 3 shows the thalweg for the total length of the table of Exp1a and the corresponding profile is shown in Fig.1a. This means to me that there is an effect of the inflow and outflow section on the bed morphology (which is directly visible in Fig. 1a) which in turn may affect the results of the wavelet analysis. This needs to be evaluated. There is also a mismatch between the thalweg elevations the figures - please explain. Moreover, the thalweg is also meandering - how was this accounted for? Note also that it was mentioned that the bricks represent a linear reference elevation. Looking at the colors of the bricks and the color-scale of Fig. 3 I would actually disagree with this statement (note also that no units are given for the scale). Another comment concerns the wetted width which, according to the numbers presented in Table 2, was different, even for bankfull conditions. I calculated the wetted width for Exp1c(3) from the numbers presented in Table2 and the formulas given at L143 and 144 and obtained a wetted width of 0.32 m which is larger than the channel width of 0.30 m. How is that possible? This in turn raises some serious questions regarding the accuracy of the experimental data which needs to be discussed in much more depth given the small scale of the experiments (see also my comment regarding the surface tension). This, together with the influence of the inlet and outlet sections indicates that more work is required to substantiate the results of the study.

Author: We do not agree with the comment regarding the effect of the channel boundary on the wavelet transform or the broader results that are presented. The concavity of the thalweg elevation profile appears greater due to the vertical exaggeration, and the effects of the inlet/outlet are both minor and spatially localized. Thus, the removal of the edges (1 m upstream and downstream) does not change the results of the wavelet analysis, and therefore, the predicted values of k_s are approximately the same (Figure 1). The edges do not matter because (1) the concavity is immediately removed by the longest wavelength of the wavelet transform, and thus, does not affect the other wavelengths, (2) this very long wavelength has the smallest contribution to the roughness length, and (3) the profile is sufficiently long and has five

uninterrupted pool-riffle pairs, such that whatever influence the edges have is averaged out and does not affect the results of the analysis. Also, no water surface gauges are placed within 60 cm of the upstream or downstream ends to minimise edge effects on the hydraulics, which has been noted in the revised methods section.

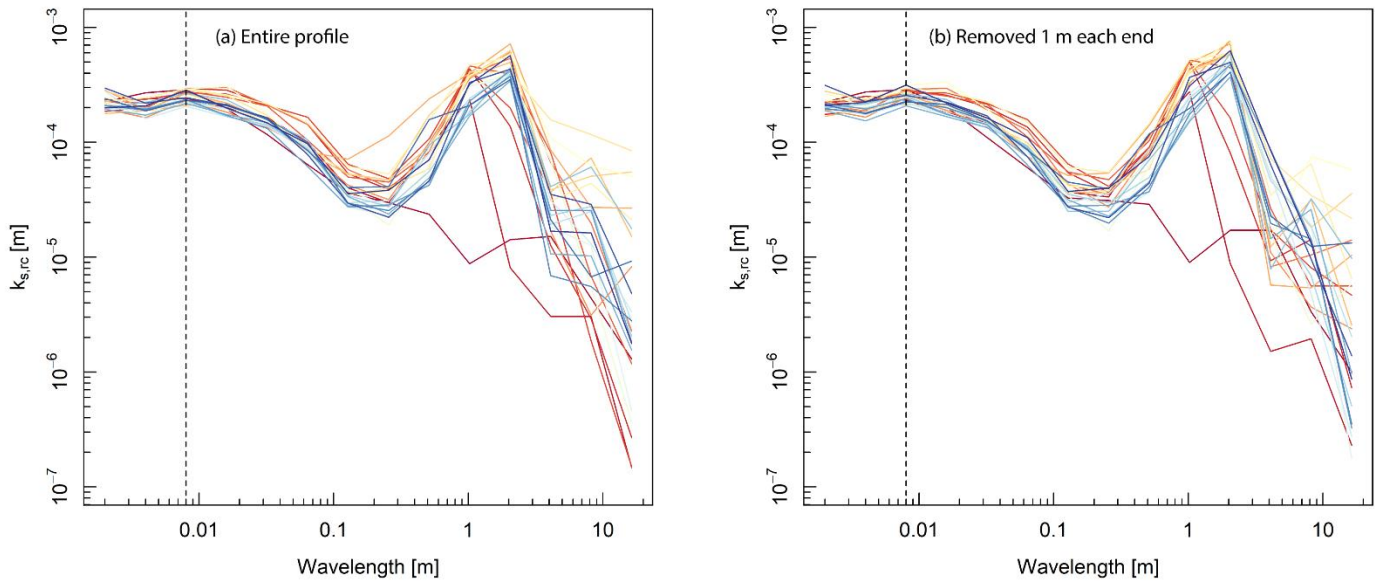


Figure 1. Drag size distribution when (a) entire profile is used, and (b) 1 m is removed off the end of each profile. Note the alteration of $k_{s,pred}$ to $k_{s,rc}$ in the new figure.

We do not understand what is meant by "accounting for meandering", and do not see a mismatch between the thalweg elevations and the figures. The elevations have been extracted from the DEM directly using the estimated position of the thalweg, the process for which is described in L140-141. If there is indeed a mistake, however, we are keen to correct it.

We agree and have clarified that the bricks are not a perfectly linear reference elevation, but it is worth noting that they do not need to be. The elevation of the brick tops varies by plus-minus 4 mm in elevation across the ~ 11 m of the experiment, but the distribution of heights centers around an average elevation, which then provides the appropriate reference for detrending the model. This has been clarified in the text. Units are present within the DEM figure, note the "m" next to the zero.

The minor discrepancy in wetted width calculations was a result of an error in the averaging of velocity values, which has now been resolved (there is almost no change in the reach-averaged values). It is also noted that there is a slight variation in the width of the model around the 30 cm target (plus-minus a centimeter or so, as noted in the text), and back-calculated values of wetted width may vary between ~0.29 and ~0.3 cm.

Reviewer: L149: What was the range of the discharges and what was the grain-size distribution of the bed material?

Author: We have included the range of discharges used in Hohermuth and Weitbrecht (2018) and a summary of their grain size distribution.

Reviewer: L157: Strictly speaking, drag is not estimated. What is estimated is k_s , a roughness length.

Author: Agreed, and we have made corrections throughout changing "drag" to "roughness length".

Reviewer: L159: Since skewness plays an important role, it would be good to show corresponding distributions.

Author: We agree, and the decomposition of skewness and a brief description has been included.

Reviewer: L166: What exactly is meant by "diversity of roughness peak heights"? This remains unclear.

Author: The diversity of roughness peak heights means the variability in the elevation of the peaks of roughness elements. If there is diversity, then the roughness elements have different heights (i.e. dune crests will be at different elevations). This explanation has been added to the text.

Reviewer: L174: I see five peaks in the profile in Fig.1 - this number is not sufficient? (I acknowledge my comment above regarding the influence of the inflow and outflow section). Nonetheless, this needs to be discussed in more detail.

Author: The number of pool-riffle pairs is sufficient based on the figure and discussion of edge effects provided above.

Reviewer: L175: What was the range of delta in the present investigation?

Author: We have clarified that the delta parameter is the vertical range of peak heights divided by the mean. Values of delta are generally over 1 and may reach as high as 4 (over the 0.35 threshold identified by Forooghi et al. 2017) for the topographic wavelengths in the present investigation. The longest 3-4 wavelengths (over 2 m) do not contain enough peaks for delta to be calculated. We have provided some statistics on delta values in the revised manuscript.

Reviewer: L178: I do not understand Figure 7 from the previous presentation of the material.

Author: We have removed this sensitivity analysis as it was confusing and unnecessary.

Reviewer: L179: But k_s is a length scale which is different from drag. Please clarify.

Author: As above, this has been clarified.

Reviewer: L190: I assume that the profile was detrended for the analysis, i.e. the bed slope is not considered in this analysis? L197: What is meant by $k_{s,pred}$? How was this determined?

Author: We have clarified the detrending process and the calculation of $k_{s,pred}$ in the methods. Bed slope is not considered in the roughness correlation. No detrending is required for the TRC approach given that the wavelet transform removes the overall trend. However, when applying the roughness correlation to the profile without the transform (to obtain $k_{s,pred}$), a linear detrend is first applied. We will note that ' $k_{s,pred}$ ' refers to the predicted k_s value for an individual wavelength, which is consistent with its usage elsewhere in the manuscript.

Reviewer: L201: It is stated that topographic variation tends towards zero, but above (L191) it is stated that the effective slope is greatest at grain-scale wavelengths (this could also be seen as a measure of topographic variation at another scale). This is contradictory in my opinion. Please explain.

Author: This may appear contradictory perhaps due to the language used. The effective slope is indeed greatest at the grain-scale wavelengths as the oscillations are tightly bunched, however, these wavelengths don't have a great deal of height variation (we used the term 'topographic variation' here, which may have confused). Effective slope is related to the aspect ratio of roughness elements rather than their vertical height. Thus, despite the pool-riffle sequence having a greater amplitude than individual grains, it has a low effective slope. We have clarified in the text.

Reviewer: L024: This figure is the same as the Form Size Distribution proposed by Nyander et al (2003)? How is it possible that it is the same? Please be more specific.

Author: The type of graph is the same but the data is different. Nyander et al. (2003) used a wavelet transform to show how topography varies across different scales in a gravel-bed flume. This has been clarified.

Reviewer: L205: I am confused now. Here it is stated that Equation 1 is used to predict k_s , which is ok. But what is then the relative value of $k_{s,pred}$ (see L 197)? I also see the need to define the concept of determining k_s for different wavelengths from a hydraulic point of view in more detail taking the physics into account (and the assumptions on which the determination of k_s is based: For example, were local values of velocities and slopes used? How was it ensured that uniform flow conditions prevailed? What about 2D-flow conditions at the grain scale? Don't get me wrong, the presented results are certainly interesting, but this needs to be elaborated in much more depth in my opinion.

Author: By relative values we mean, it may be more valid to make comparisons for a given river, as opposed to making comparisons across different hydraulic conditions. This has been explained more clearly. Local values of velocities and slopes were not used, and we do not assume uniform flow conditions given that the model has morphologic elements that give rise to a spatial distribution of velocity. We have addressed the comment regarding the physics of the decomposition above and would welcome further discussion as there has been no sufficient answer presented in the literature.

Reviewer: L213: The DEM is not analyzed, but the thalweg-profile extracted from the DEM.

Author: Agreed, change has been made.

Reviewer: L214: The mother wavelet is only mentioned in the figure caption indicating the need to present the chosen approach in much more detail. This is rather confusing (also the choice of the other wavelets indicated in Figure 7 which remains a black box to me).

Author: The role of the mother wavelet has been clarified in the text along with the general description of wavelets above.

Reviewer: L218: I would argue that I only see one extreme outlier.

Author: Agreed. There is one extreme outlier, which is significant.

Reviewer: L224: I basically agree, and this would be one step towards answering my comment @L205. However, I am not sure that I understand the statement regarding the proportionality - it should give the same value

Author: The comparison of $k_{s,pred}$ and the sum of (summed) $k_{s,pred}$ is an important check, as we would expect them to have different values. The two values differ as the process of signal decomposition and recombination is characterised by wave interference. For example, for each thalweg elevation profile there are two estimates of amplitude (1) the standard deviation of elevations, and (2) the sum of the standard deviation for each wavelength decomposed using the wavelet transform. Decomposing and recombining wavelengths alters the position and magnitude of peaks and troughs in the wavelengths, and therefore, their amplitude. Wave interference may potentially confound estimates of k_s using the wavelet transform. Therefore, it is important to check that $k_{s,pred}$ and the sum of (summed) $k_{s,pred}$ are at least positively correlated. We have added an explanation to the text.

Reviewer: L226: I still do not understand exactly how $k_{s,pred}$ was obtained. What is meant without the transform? Does that mean the overall profile was used? This needs to be described in much more depth.

Author: This is correct, we can clarify: "...obtained by applying the roughness correlation to the elevation profile without the transform (i.e. using the raw thalweg elevation profile)." The explanation has been restructured and added to the methods instead.

Reviewer: L229: Why does that validate the TRC approach? The numbers deviate (see my comment @L224). A comment in between - all this compares (to my understanding) the presents results in regard to the approach of Forooghi et al. (2017) - but how does that approach relate to the real k_s value? That means what is the "real" k_s value from the experiments? This needs to be discussed in depth. It seems that the hydraulic data have not been used to determine k_s (I might be wrong here, but this indicates that a more precise presentation of the material is required).

Author: The reviewer is correct; we did not initially calculate the k_s value using the hydraulic data but we have now added this analysis to the manuscript. Upon this recommendation, we calculated the k_s value using the hydraulic data and the rough-flow form of the Colebrook-White equation, using coefficients for open-channel flow from Keulegan (1938). We then compared this estimate of k_s ($k_{s,CW}^*$) to the roughness correlation estimate (now termed [$k_{s,rc}^*$] rather than [$k_{s,pred}^*$]) (Figure 2). The experiments conducted for this study (PBR pool-bar-riffle, and PB plane-bed) have values of $k_{s,rc}^*$ that are consistently within a factor-of-two of the Colebrook-White k_s values.

In the case of the step-pool experiments, there is a significant under-prediction of k_s by the roughness correlation of around an order-of-magnitude, which may be explained by the effect of lower relative submergence (median $h/d_{84} = 1.48$, rather than 3.91). We believe that the similarity of the two estimates of k_s for the lower gradient experiments may alleviate the concerns of the reviewer regarding the assumptions of the TRC approach (use of a single profile, ignoring slope, etc.), and also helps to position estimates of k_s within a familiar framework for readers.

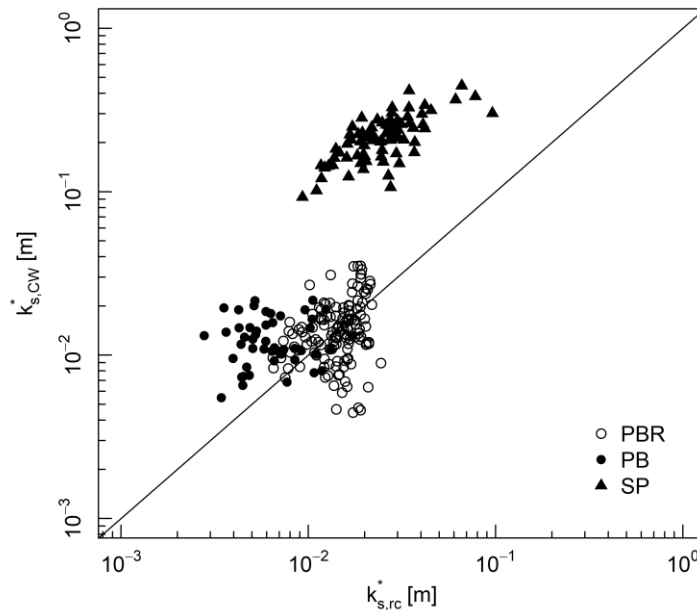


Figure 2. Comparison of k_s calculated using the Colebrook-White formula and the roughness correlation. Data has been categorized based on the morphology: PBR = pool-bar-riffle (30cm and 45cm experiments), PB = plane-bed (8cm experiments), SP = step-pool (Hohermuth experiments).

Reviewer: Figure 9: First, see my comments regarding the experimental data. Second, why is $k_{s,pred}^*$ used here and not $sum(k_{s,pred})$. This is confusing, as the latter parameter has been derived but is not presented in this final plot.

Author: I believe this will be, in part, clarified by the above explanation. $k^*_{s,pred}$ is used rather than $\sum(k_{s,pred})$ because wave interference affects the value of $k_{s,pred}$. In short, if one is interested in the decomposition of the roughness length into different scales, then the TRC approach may be used (i.e. $k_{s,pred}$ for each wavelength). However, if the total value of k_s is of interest, $k^*_{s,pred}$ should be used, which is why this value was used for the original Figure 9 (the prediction of total flow resistance).

Reviewer: L251 and following: This main information here should have been presented in the introduction in my opinion.

Author: There may be an argument for this structure. However, we suggest that the implications for geomorphology are more appropriately located at the end. Based on comments from another reviewer, we have strengthened this discussion and added a range of potential applications.

Reviewer: L268 and following: Please consider my above comments. References: The short communication is overloaded with references

Author: We have removed several references from the manuscript.

Reviewer 2 responses and changes

General comments

We would like to thank the reviewer for suggesting where communication could be enhanced, and for encouraging us to consider the broader implications and applications of our research.

Reviewer: In the present study, only one single longitudinal profile is analysed. Although it is mentioned that “multiple streamlines (parallel or even intersecting) could be employed”, I think that this aspect should be discussed in more detail. For example, how much would the results be affected by selecting different streamlines? How representative is a single streamline for the flow conditions averaged over the cross-section?

Author: There are two parts to this comment: (1) highlighting the limitations of the TRC approach in three-dimensional channel beds, and (2) the sensitivity of the TRC results to the position of the streamline.

We agree that a single streamline cannot be fully representative of the entire cross-section because it does not consider other resistance elements (e.g. banks, emergent bars), nor three-dimensional interactions between flow and channel topography. We suggest that, especially in simplified channels such as the ones of interest in this investigation, the thalweg elevation profile may still capture the important interactions between the channel topography and hydraulics. We would like to provide some evidence to demonstrate this.

Upon recommendation by another reviewer, we calculated the k_s value using the hydraulic data and the rough-flow form of the Colebrook-White equation (which we can treat as a ‘measured’ k_s value), using coefficients for open-channel flow from Keulegan (1938). We then compared this estimate of k_s ($k^*_{s,CW}$) to the roughness correlation estimate (now termed [$k^*_{s,rc}$] rather than [$k^*_{s,pred}$]) (Figure 3). The experiments conducted for this study (PBR pool-bar-riffle, and PB plane-bed) have values of $k^*_{s,rc}$ that are consistently within a factor-of-two of the Colebrook-White k_s values, centering around the 1:1 line. On the other hand, for the published step-pool data, there is significant under-prediction of k_s by the roughness correlation of around an order-of-magnitude, which may be explained by the lower relative submergence (median $h/d_{84} = 1.5$, rather than 3.9).

The relatively close relationship between the two independent estimates of k (estimates from either topography or hydraulics), suggests that for the experiments we conducted, the thalweg elevation profile is representative of in-channel processes. We have included this analysis and discussion in the revised manuscript.

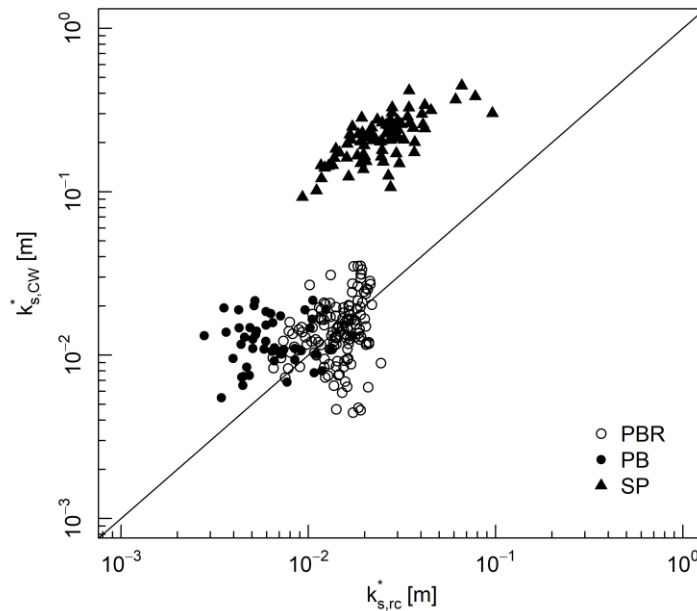


Figure 3. Comparison of k_s calculated using the Colebrook-White formula and the roughness correlation. Data has been categorized based on the morphology: PBR = pool-bar-riffle (30cm experiments), PB = plane-bed (8cm experiments), SP = step-pool (Hohermuth experiments). Note the alteration of $k_{s,pred}$ to $k_{s,rc}$ in the new figure.

Now we will discuss the sensitivity of results to the streamline position. When we were testing the analyses, we initially used a series of parallel profiles positioned from one side of the wetted area to the other. There was a significant difference in results (FSD and DSD) between the profiles, given that some were aligned with the thalweg and the pool-riffle undulations, and others captured a set of different features such as emergent bars. For the profiles positioned near the centerline, the only discernible variation in was in the amplitude of the large-scale variations, due to some profiles intersecting with the deepest parts of pools. Moreover, for these near-thalweg profiles, the estimated values of k_s showed almost the same pattern (e.g. the proportion of grain- and form-scale k_s values, general drag size distribution DSD shape). It was clear that the general results were the same if the profile intersected with the deep part of the channel cross-section.

We have included a figure showing the profiles used for Experiment 1a (Figure 4), which have been extracted using the technique detailed in the methods. There is some variation between the profiles, particularly in the depth of the pools, which may represent an actual change in morphology, or it may be due to the elevation profiles taking slightly different paths. There are even a couple of cases where the profile intersects with a bar at the very downstream end, which is an error that occurs in the profile extraction process when the topography is more complicated. However, despite these variations in profile shape, the DSD remains relatively similar once the pool-bar-riffle sequence has been formed (Figure 5a). The only changes in the k_s decomposition are at the largest spatial scales, but these contribute almost no k_s and are therefore insignificant. Even if we remove the final 1m of either end of the profiles (thus removing edge effects and potential errors), the DSD is still the same (Figure 5b).

In summary, the decomposition of k_s is not very sensitive to the precise position or shape of the profile. It is for this reason that we are currently exploring the DSD as an index of channel character, given that different broad types of

channel morphology (pool-riffle, plane-bed, step-pool, dune-ripple, etc.) seem to manifest as distinctive distributions of k_s as a function of scale.

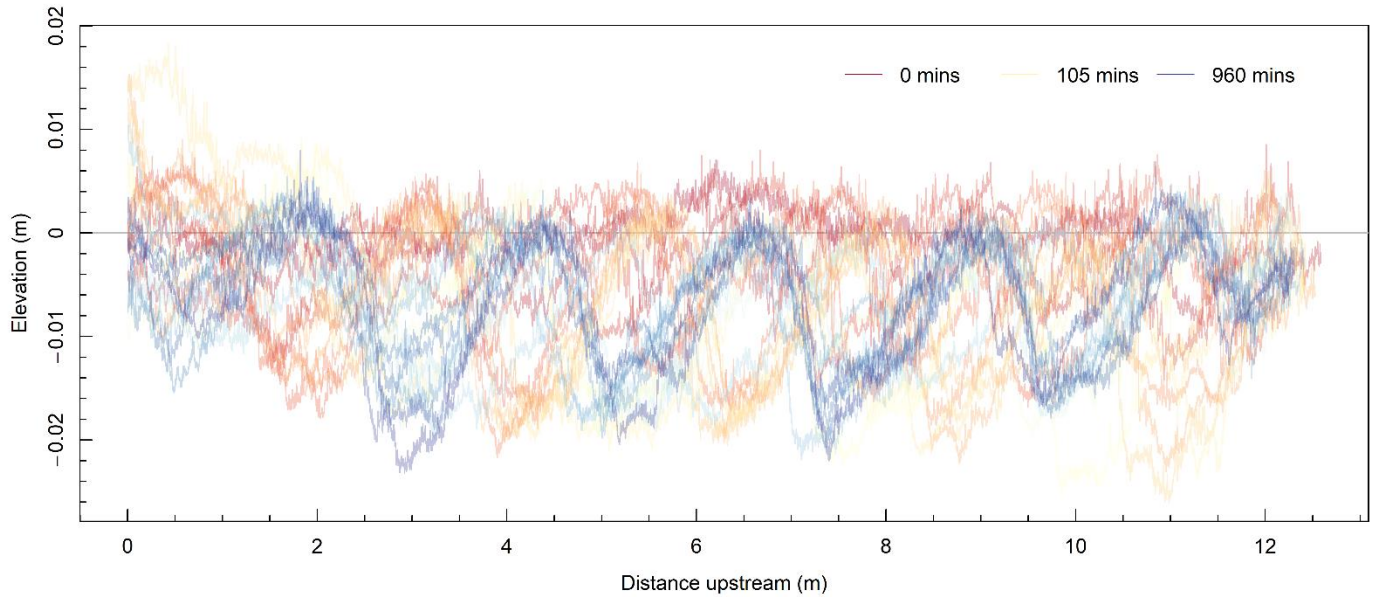


Figure 4. Thalweg elevation profiles (based on estimated position) throughout Experiment 1a. Zero represents the mean elevation of the screeded bed.

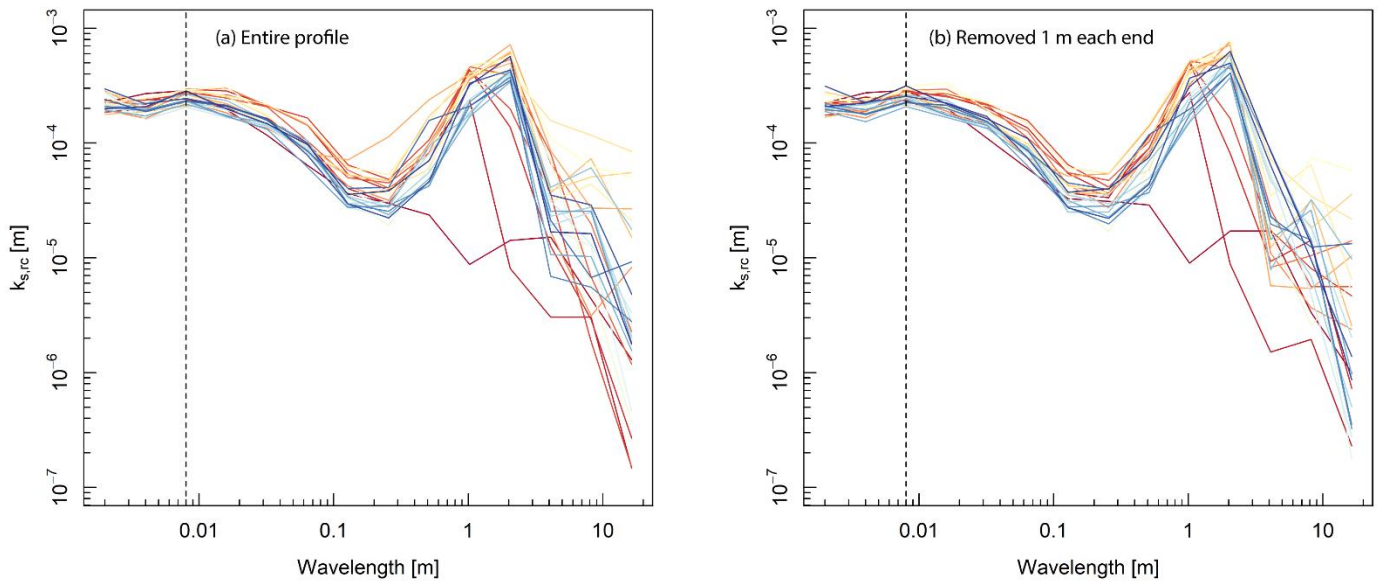


Figure 5. Drag size distribution when (a) entire profile is used, and (b) 1 m is removed off the end of each profile.

Reviewer: Frequent reference is made to the study of Forooghi et al. (2017), but for readers unfamiliar with this study it is not always clear what is meant exactly or what meaning, for example, the term “effective slope” had in this cited study (see also my specific comment below to L160-178). Therefore I suggest providing some more information on this important background study.

Author: We agree that more information regarding the initial study and effective slope parameter may be important. For example, we will explain in more detail the development of the roughness correlation in Forooghi et al. (2017), such as

the general approach (i.e. relating different metrics of surface geometry to the total ks), and the surfaces that were used (e.g. their general characteristics). The effective slope is potentially a source of confusion given that surfaces with a high effective slope (i.e. steep roughness elements) do not necessarily have a large range of elevations. We have taken steps to explain this by improving word-choice and using examples.

*Reviewer: The application of the TRC approach to the two different sets of flume experiments as illustrated in Figure 9 appears to result in a somewhat better flow resistance prediction than more traditional approaches (reduced root-mean-square error when using the $k^*_{s,pred}$ roughness measure as compared to using the σ_z measure), if the measure $k^*_{s,pred}$ really refers to the application of the new TRC approach. However, it is not clear how $k^*_{s,pred}$ was calculated, this needs to be clarified.*

Author: The $k^*_{s,pred}$ parameter is calculated by applying the roughness correlation in the way Forooghi et al. (2017) originally intended, that is, the relation is applied directly to the profile without any use of the wavelet transform. We have clarified this in more detail in the methods section of the revised manuscript.

Reviewer: The presence of large wood on the streambed can substantially alter the total resistance, and that particularly in such a situation using σ_z as compared to using e.g. a characteristic grain size such as D_{84} improves flow resistance calculations. Can you speculate if and how using the TRC approach could further improve flow resistance calculations in such settings?

Author: We agree that this is an important consideration. Given that the TRC approach uses surface geometry alone, any features on the channel bed surface (live or dead vegetation, large immobile grains, human structures) are incorporated within the estimates of ks. Isolating the role of large wood could be achieved with some creative thinking. For example, using structure-from-motion datasets of mountain channels, one could classify areas of large wood, remove them, and then re-interpolate to create a seamless bed without any wood. The TRC analysis could be applied to both the original DEM and the wood-less DEM (using perhaps a set of parallel profiles). The difference in ks could be attributed to the influence of large wood.

One could also perform the reverse by adding roughness elements to a profile to estimate the corresponding increase in flow resistance. This technique has applications in engineering (stabilization, flood-risk analysis) and re-naturalisation (geomorphic and biological), of rivers. We will be providing a brief discussion of these potential applications in the revised manuscript.

Reviewer: I see one potentially interesting further application of the TRC approach with regard to the question of stress partitioning in gravel-bed streams which is one important approach to improve bedload transport predictions in these channels (e.g. Ancey, 2020, JHR, part 2, <https://doi.org/10.1080/00221686.2019.1702595>). Some discussion of this aspect would be welcome.

Author: We are familiar with the concept of shear-stress partitioning but have yet to directly consider the application of the TRC to this problem. From our understanding, stress-partitioning is necessary to make accurate predictions of sediment transport because only grain drag acts to move sediment, and form drag dominates the momentum budget. A common approach to determining form drag is to subtract grain drag from the total stress, where grain drag is calculated using empirical relations (usually sourced from flume experiments with flat, planar beds, and using some representative roughness value). The TRC approach provides a more direct means of partitioning drag across different scales. However, one of the key limitations here is that the TRC approach, in its current form, does not incorporate the effects of slope or relative roughness (it assumes a flat surface as well as fully-developed flow), which are especially important in bedload transport processes. We have included a discussion of this topic in the revised manuscript.

Specific comments

Reviewer: Figure 1b): indicate which line refers to grain and form wavelength.

Author: We have used a dashed line for the form wavelength.

L160-178: In the process of selecting an appropriate correlation between roughness measures and elements of the wavelet analysis, the authors refer to the study of Forooghi et al. (2017) who used a variable called “delta” (a measure of the diversity of roughness peak heights), and report that “effective slope is approximately proportional to drag in the range $0 < ES < 0.35$ ”. It is not clear whether the authors also determined “delta” or not. Furthermore, in eq. (2) a critical value of $\delta = 0.35$ is used to separate the two ranges, whereas later in the text a (critical) value of 0.35 is associated with ES. (L172). This is all somewhat confusing and requires clarification.

Author: We agree that this is important to explain. We have clarified that the delta parameter is the vertical range of peak heights divided by the mean. By identifying peaks in each wavelength, we found that delta was generally over 1 for our experiments and was as high as 4 (over the 0.35 threshold identified by Forooghi et al. 2017). The longest 3-4 wavelengths do not contain enough peaks for delta to be calculated. We have included some statistics on delta values in the revised manuscript.

A critical value of ES has been identified to be 0.35, which separates two regimes, termed ‘waviness’ and ‘roughness’ (Schultz & Flack, 2009, “Turbulent boundary layers on a systematically varied rough wall”). In the waviness regime, where $ES < 0.35$, there is a positive correlation between ES and the roughness length (that is if the height range of the roughness remains the same and the aspect ratio changes). In the roughness regime, ES has far less effect on the roughness length. The 0.35 thresholds for both ES and Delta appear to be a coincidence. This has been clarified.

Reviewer: Figure 4: If the vertical dashed line is meant to indicate D_{max} , it should plot at 0.008 m (L102).

Author: We picked this up after submission and have corrected.

Short communication: Multiscalar ~~drag~~ roughness-length decomposition in fluvial systems using a transform-roughness correlation (TRC) approach

David L. Adams^{1,2} and Andrea Zampiron³

¹Department of Geography, The University of British Columbia, Vancouver, BC, Canada

²School of Geography, The University of Melbourne, Melbourne, VIC, Australia

³Department of Mechanical Engineering, The University of Melbourne, Melbourne, VIC, Australia

Correspondence: David L. Adams (dladams@alumni.ubc.ca)

Abstract.

In natural open-channel flows over complex surfaces, a wide range of superimposed roughness elements may contribute to flow resistance. Gravel-bed rivers present a particularly interesting example of this kind of multiscalar flow resistance problem, as both individual grains and bedforms ~~can potentially be important roughness elements~~ may contribute to the roughness length. In this paper, we propose a novel method of estimating the relative contribution of different physical scales of river bed-in-channel topography to the total dragroughness length, using a transform-roughness correlation (TRC) approach. The technique, which requires only a single longitudinal profile, consists of (1) a wavelet transform which decomposes the surface into roughness elements occurring at different wavelengths, and (2) a ‘roughness correlation’ that estimates the drag-roughness length (k_s) associated with each wavelength based on its geometry alone, ~~expressed as k_s . We apply the TRC approach. When~~ applied to original and published laboratory experiments ~~and show that the multiscalar drag decomposition yields estimates of grain- and form-drag that are consistent with estimates in channels with similar morphologies. Also, we demonstrate that with a range of channel morphologies,~~ the roughness correlation ~~may be used to estimate total flow resistance via a conventional equation, suggesting that it could replace representative roughness values such as median grain size or the standard deviation of elevations. An improved understanding of how various scales contribute to total flow resistance may lead to estimates the total~~ k_s to within a factor-of-two of measured values but may perform poorly in very steep channels with low relative submergence. The TRC approach provides novel and detailed information regarding the interaction between surface topography and fluid dynamics that may contribute to advances in hydraulics ~~as well as,~~ bedload transport, and channel morphodynamics.

1 Introduction

Understanding flow resistance is of great interest to river research and practice. The estimation of flow resistance is important for determining flood magnitudes, predicting ecological habitat, ~~and understanding the morphodynamic behaviour of channels~~ estimating rates of sediment transport, and understanding channel morphodynamics. However, the hydraulics of gravel-bed channels, in particular, are relatively poorly understood ~~due to a range of factors~~ (see Ferguson, 2007). Given

that most of the foundational work in fluid dynamics, upon which conventional approaches to predicting flow resistance are based, was conducted using regular (e.g., Schlichting, 1936) or uniscalar (e.g., Nikuradse, 1933) bed geometry, the multiscale topographic characteristics of these rivers presents a major challenge. In particular, ~~both individual grains and bedforms on the bed surface, spanning orders-of-magnitude of scale, may contribute have variable contributions to the total flow resistance (see Adams, 2020a). Researchers have been aware of these limitations for over half-a-century (Sundborg, 1956; Leopold et al., 1964) and have used empirically derived coefficients to account for the multiple scales of roughness present (Chow, 1959; Hey, 1979) although such an approach has considerable limitations (Ferguson, 2007; Adams, 2020a). There have also been more mechanistic attempts to disaggregate flow resistance, primarily across different channel types. Thus, moving forward, mainstream empirical approaches to estimating flow resistance based solely on grain diameter would ideally be replaced by approaches that explicitly account for multiple spatial scales (see Adams, 2020a). Decomposing roughness lengths into different scales may contribute to an understanding channel morphodynamics given that energy dissipation is increasingly recognised as a condition governing system behaviour (Eaton and Church, 2004; Nanson and Huang, 2018; Church, 2015). Also, the partitioning of bed stresses between grain and form scales is an important step in predicting bedload transport (Ancy, 2020).~~

Inspired by early work in fluid dynamics (Schlichting, 1936; Keulegan, 1938) and subsequent work in fluvial hydraulics (Einstein and Banks, 1950; Nowell and Church, 1979), some geomorphologists sought to disaggregate the roughness length into 'grain' (small-scale) and 'form' (large-scale) components (Parker and Peterson, 1980; Prestegard, 1983; Hey, 1988; Weichert et al., 2000).

Contributions by correlating bar geometry with flow resistance (Davies and Sutherland, 1980; Prestegard, 1983). However, further work was likely hindered by limitations associated with the collection of topographic data in rivers (Furbish, 1987; Robert, 1988). Advances in remote-sensing and statistics have since allowed researchers to explore detailed scaling characteristics of gravel-bed surfaces using ~~structure functions (Furbish, 1987; Robert, 1988, 1991; Clifford et al., 1992), filtering (Bergeron, 1996), analyses such as variograms (Robert, 1988; Clifford et al., 1992) and transforms (Nyander et al., 2003). This approach to analyzing river beds has~~ Topographic analyses have led to multiscale decompositions of geometric roughness, rather than direct in rivers, although to our knowledge, full decompositions of hydraulic roughness have not yet been presented. The latter approach has been developed for complex aeolian surfaces using transforms (Nield et al., 2013; Pelletier and Field, 2016; Field and Pelletier, 2018), which serves as a proof-of-concept for ~~the multiscale drag decomposition approach~~ a multiscale roughness length decomposition.

Also, as high-resolution spatial information becomes increasingly available to geomorphologists working in both laboratory and field environments (Westoby et al., 2012), there is a general need for statistical representations that effectively summarise these large datasets in a way that is informed by theory. Moreover, as energy balance is increasingly recognized as a condition governing channel behaviour (Eaton and Church, 2004, 2009; Nanson and Huang, 2008, 2018; Church, 2015), improved understanding of flow resistance may contribute to a broader understanding of fluvial systems.

In a review of flow resistance in gravel-bed rivers, Adams (2020a) identified two relatively recent advancements in the fields of statistics and fluid dynamics that could contribute to a multiscale drag-roughness length decomposition tool. The first advancement is the wavelet transform, which is generally superior to the Fourier transform when analysing the un-

derlying structure of complex and aperiodic signals, ~~due to its~~. This is due to the use of a finite analysing function ('the wavelet') (rather than a continuous ~~one~~) wavelet function, that gives rise to a family of wavelets that are dilated (stretched and compressed) and translated (shifted) along the signal (Torrence and Compo, 1998). There are now various types of wavelet transform suited to different applications, some of which have been applied in rivers (Kumar and Foufoula-Georgiou, 1997; Nyander, 2004; Keylock et al., 2014). The second advancement is the development of roughness correlations for irregular surfaces ~~(e.g. Forooghi et al., 2017)~~(e.g. Forooghi et al., 2017; De Marchis et al., 2020), which estimate the ~~fluid drag generated by roughness length of~~ a surface based purely on its geometric characteristics.

65 In this ~~piece~~study, we present a novel method of estimating the relative contribution of different physical scales of river bed topography to the total ~~drag~~roughness length, using only a single longitudinal profile. The general approach consists of (1) a wavelet transform in which the channel surface is decomposed into a set of more simple components each at a different wavelength, and (2) a roughness correlation that estimates the ~~drag~~roughness length associated with each wavelength, which is expressed as the equivalent sand roughness parameter k_s (Nikuradse, 1933; Schlichting, 1936). By modifying the specific roughness correlation that is used, the transform-roughness correlation (TRC) approach may be applied ~~in across~~ a wide range of ~~channel types and~~ hydraulic conditions. To demonstrate ~~this tool, we present code in R language and the TRC analysis,~~ we apply it to a series of original laboratory experiments with high-resolution digital elevation models (DEMs), as well as some additional published data. ~~Multiscalar drag decomposition provides researchers with useful information as they approach challenges pertaining to flow resistance and channel morphodynamics.~~

75 2 Methodological considerations

The transform-roughness correlation approach is a generic tool that should be adapted based on the hydraulic conditions and the purpose of its application. These considerations should span the ~~data that is used~~dataset, the type of wavelet transform, and the specific roughness correlation that is selected. We first discuss these general considerations ~~first as they provide to provide important~~ context for the TRC approach, prior to introducing the experimental data and the Forooghi et al. (2017) roughness correlation in Section 3.2.

80 First, the minimum resolution and spatial extent of the topographic dataset should be informed by the scale of the features of interest. The data should have a sufficiently ~~small~~high spatial resolution such that it can capture the range of ~~bed features that contribute to in-channel features that produce~~ drag. Also, to capture the characteristic geometry of bed features ~~-(notably, height and spacing) and estimate a reach-averaged roughness length,~~ the spatial extent of the dataset should be at least the length of the largest features that ~~produce significant drag~~significantly affect the flow, for example, it should span ~~many dunes a series of dune~~ crests or pool-riffle pairs.

Second, given that ~~hydraulic roughness~~the hydraulic roughness of in-channel features is of interest, the ~~data could channel topography can~~ be reduced to ~~streamlines representing primary flow paths. In some contexts, it may be acceptable to simplify the in-channel area to~~ a one-dimensional profile extending along the thalweg, ~~given that this should represent the surface that most of the flow interacts with. Alternatively, if the~~ representative of the primary flow path. It is important to note here that

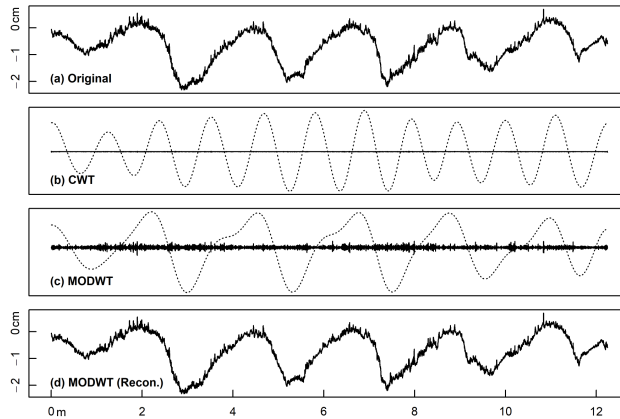


Figure 1. a) Thalweg elevation profile at end of Experiment 1a (this study) featuring a prominent pool-riffle sequence, where the x-axis represents distance upstream, b) grain ($\lambda = 4$ mm) and form ($\lambda \approx 2$ m, dashed line) wavelengths derived from CWT, c) the same two wavelengths derived from a MODWT, and d) the original signal reconstructed from the MODWT by recombining wavelengths.

this approach ignores resistance elements such as channel planform, and three-dimensional interactions between flow and in-channel topography. If both hydraulic and topographic data are available, this assumption may be validated by comparing the roughness length estimated using the roughness correlation to a measured roughness length (see Section 3.1.2). If the range of interactions between the flow and the surface is of interest, multiple streamlines (parallel or even intersecting) could be employed parallel elevation profiles could be analysed.

Third, the choice of wavelet transform in this context between discrete and continuous wavelet transforms (DWT and CWT) is a trade-off between the resolution of the decomposition and the ability to interpret it. The maximal overlap discrete wavelet transform (MODWT) offers several advantages over the discrete wavelet transform (DWT) and facilitates alignment between the original signal and the decomposition. The continuous wavelet transform (CWT) physical resemblance to the original profile. Compared to the DWT, the CWT extracts more intricate structural characteristics from the original data signal and yields a greater number of wavelengths between which information is shared (Addison, 2018). However, the redundancy in the CWT generates a more abstract representation of the topographic variation at a given wavelength. A comparison of In Figure 1, we compare wavelengths extracted using MODWT and CWT methods is presented in Figure 1 a maximal overlap discrete wavelet transform (MODWT) and a CWT using the same elevation profile. At the wavelength corresponding to the spacing of a pool-bar-riffle sequence ($\lambda \approx 2$ m), the MODWT is oscillations output by the MODWT are aligned with the original thalweg elevation profile pool-riffle undulations (i.e. the position of peaks and the general shape are similar), but the CWT is not oscillations do not appear to align with the original profile. Given that the CWT wavelengths they do not resemble the original data, interpreting the results of roughness correlation applied to these wavelengths may be more difficult, and such results may be entirely invalid channel surface, it may be invalid to infer hydraulic behaviour from CWT wavelengths.

Fourth, the specific roughness correlation that is used should match the regime of the channel's boundary Reynolds number $Re^* = U^*k/v$, where U^* is shear velocity, k is some representative roughness scale, and v is kinematic viscosity. Given that the

fluid-dynamics characteristic of different boundary Reynolds numbers are highly varied, roughness correlations have only been developed for relatively limited ranges of Re^* . For example, given that gravel-bed rivers tend to be within the fully rough regime where $Re^* \geq 70$ (Buffington and Montgomery, 1997; Schlichting, 1979), it may only be valid to apply roughness correlations obtained for that regime specifically. Also, the flow should be turbulent, and it should be two-dimensional, ~~indicated~~ which may be indicated (although not guaranteed) by flow aspect ratios (w/h , where w is the wetted width and h is flow depth) greater than 5 (Nezu and Nakagawa, 1993).

Last, roughness correlations in fluid dynamics tend to be developed for flows sufficiently deep to have logarithmic velocity profiles, which should be considered when they are applied to flows with less developed profiles. Jimenez (2004) suggested that logarithmic layers develop where relative submergence h/k is greater than 40, although Cameron et al. (2017) observed a logarithmic layer in rough open-channel flow at submergences as low as 1.9. During most flow conditions, it is common for gravel-bed rivers to have relative submergences of less than 10, and in some cases, as low as 0.1 (Lee and Ferguson, 2002; Ferguson, 2007), where no logarithmic layer can develop because roughness elements are not submerged. However, if one is interested in channel-forming flows capable of reworking the bed surface (Ashworth and Ferguson, 1989; Wolman and Miller, 1960) where relative submergence may be two orders of magnitude higher (~~Limerinos, 1970; Griffiths, 1981; Bray, 1982; Millar, 1999~~) (Limerinos, 1970; Bray, 1982), the logarithmic assumption should be satisfied for most rivers.

3 Application of TRC approach in gravel-bed rivers

3.1 Stream table experiment

To demonstrate the TRC approach, we required a large set of DEMs and associated hydraulic data for validation, and ideally straight channels where in-channel features represent the dominant source of drag. We conducted a set of experiments using the Adjustable-Boundary Experimental System (A-BES) at the University of British Columbia (Figure 2). The A-BES comprises a 1.75 m wide by 12.2 m long tilting stream table, and a recirculating water pump controlled by a digital flow meter. The experiments were run as generic Froude-scaled models with an initial bed slope of 2 percent and a length scale ratio of 1:25, based on field measurements from steep gravel-bed rivers in Alberta, Canada. The bulk material ranged from 0.25 to 8 mm (~~D_{max} – D_{max}~~), with a ~~D_{50} – D_{50}~~ of 1.6 mm and ~~D_{90} of 3.9 mm (see MacKenzie and Eaton, 2017). The banks were lined with roughly-cast interlocking concrete bricks to make a straight channel. Ten stream gages were equally spaced along the inner edge of the bricks~~ D_{84} of 3.2 mm (see MacKenzie and Eaton, 2017), and the grain size distribution (GSD) is included in Figure 6.

3.1.1 Experimental procedure

~~The~~ Roughly-cast interlocking concrete bricks were configured to make two straight channels of different widths: (1) a 30 cm wide configuration that represents the scaled bankfull width of the field prototype, and (2) an 8 cm wide configuration



Figure 2. Adjustable-Boundary Experimental System (A-BES) at the University of British Columbia, showing the camera rig and the 30 cm wide channel configuration.

Table 1. Summary of experimental conditions in the A-BES. Length refers to the median length of DEMs, which generally varies by ± 0.1 m, and does not include approximately 20-30 cm of bed at the upstream end. The DEM count excludes the screeded bed which has no associated hydraulic data.

Run	Width W (m)[m] ($\pm 0.020.015$)	Length [m]	Discharge Q ([L/s]) (± 0.03)	Duration (hrs)[hrs]	DEMs	Morphology
Exp1a	0.3	<u>10.8</u>	1.5	16	24	<u>PBR</u>
Exp1b	0.3	<u>10.7</u>	1.0	16	24	<u>PBR</u>
Exp1c	0.3	<u>11.0</u>	0.67, 1.0, 1.5, 2.25	8, 4, 4, 4	68	<u>PBR</u>
Exp2a	0.08	<u>8.7</u>	0.4	16	24	<u>PB</u>
Exp2b	0.08	<u>8.6</u>	0.27	16	24	<u>PB</u>

which was selected based on preliminary experiments where channel width was decreased until bar formation was suppressed entirely. Thus, the two widths yield a range of bed morphologies and hydraulic conditions.

A set of experiments were carried out for each configuration (Table 1), yielding two broad types of in-channel morphology:
 145 (1) pool-bar-riffle (PBR), consisting of a gently meandering, undulating thalweg with alternate bars, and (2) plane-bed (PB),
with no discernible morphology beyond the grain-scale. The first experiment ('a') consisted of a bankfull equivalent flow
 for the prototype for 16 hours, where the discharge was scaled with the width of the experimental channel W . The second
 experiment ('b') consisted of a flow two-thirds of the bankfull equivalent for 16 hours. The third experiment ('c'), conducted
 for the 30 cm wide channel only, consisted of low flow for 8 hours, and then three 4 hour phases with discharge increasing by
 150 a factor of 1.5 each time.

Before each experiment, the bulk material was hand-mixed to minimize downstream and lateral sorting, and the channel area
 was screeded to the height of the weirs at the upstream and downstream end. The flow was run at a low rate (at which there
was little-to-no movement of sediment) until the bed was fully saturated, and was then rapidly increased to the target flow.

155 At the downstream end, where water free-falls over the weir, there is slight and localised lowering of the water surface due to a downdraw effect, but no discernable backwater. Each period of constant discharge was divided into phases of increasing duration, between which the bed was ~~drained and photographed~~ rapidly drained to minimise the potential for morphologic change, photographed, and re-saturated before resuming the experiment. Phases for the 16-hour experiments consisted of 5, 10, 15, 30, 60, and 120 minutes, with four repeats of each. The 4 and 8 hour periods of constant discharge followed the same sequence but did not include the longest phases. In the final 30 seconds of each phase, the water surface elevation was recorded
160 at each gage to the nearest 1 mm. ~~Given that most of the maximum flow depths that were measured were greater than 15-20 mm, this degree of precision yields errors of approximately ± 10 percent~~ Water gauges were read at an almost horizontal angle, which in conjunction with the dyed blue water, minimised systematic bias towards higher readings due to surface tension effects.

The camera rig consisted of five Canon EOS Rebel T6i DSLRs with EF-S 18-55 mm lenses positioned at oblique angles in
165 the cross-stream direction to maximise coverage of the bed, and five LED lights. Photos were taken in RAW format at 20 cm intervals, yielding a stereographic overlap of over two-thirds. Throughout the experiment, sediment collected in the trap was drained of excess water, weighed wet to the nearest 0.2 kg, placed on the conveyor belt at the upstream end, and recirculated at the same rate it was output. Zero sediment was fed into the system during the first 5-minute phase. For the five- and ten-minute phases, recirculation occurred at the end of the phase, and for the phases of longer duration, recirculation occurred every 15
170 minutes regardless of whether the bed was drained.

3.1.2 Data processing

Using the images, LAS point clouds were produced with Agisoft MetaShape Professional 1.6.2 at the highest resolution, yielding an average point spacing of ~~less than 0.5~~ around 0.25 mm. Twelve spatially-referenced control points (and additional unreferenced ones) were distributed throughout the A-BES, which placed photogrammetric reconstructions within a local
175 coordinates system and aided in the photo-alignment process. The point clouds were imported into RStudio where inverse distance weighting was used to produce DEMs at 1 mm horizontal resolution. Despite the use of control points, the ~~DEM~~ DEMs contained a slight arch effect whereby the middle of the model was bowed upwards. This effect was first quantified by applying a quadratic function along the length of the bricks, which represent ~~a~~ an approximately linear reference elevation (brick elevations vary by ± 4 mm). The arch was then removed by determining correction values along the length of the DEM
180 using the residuals, which were then applied across the width of the model.

At two points in time across the experiments, Exp1a T60.1 (5 hrs 0 min) and Exp1c Phase 2 T30.3 (3 hrs 30 min), due to errors during photo collection or the photogrammetry processing, the DEMs were slightly shorter at the upstream end (9.4 and 7.9 m in length, respectively). These DEMs were still sufficiently long to include most of the bed topography and stream gauges, and have been included in the following analysis.

185 The channel thalweg for the wide experiments was determined by first locating pool centroids using the lowest ten percent of elevations at each cross-section, and then using Gaussian kernel regression to smooth vertices between the centroids. An

example of the estimated thalweg location is shown in Figure 3. Given the absence of bars, the thalweg elevation profile of the narrower experiments was assumed to be the channel centerline.

190 By determining the position of stream gauges within the DEM, ten wetted cross-sections were reconstructed using the water surface elevation data (assuming a relatively horizontal water surface elevation), which were then used to estimate reach-averaged hydraulics. Mean hydraulic depth was calculated as $h = A/w$, where A is cross-sectional area and w is the wetted width. Velocity was estimated using the continuity equation $U = Q/A$. Shear velocity is $U^* = \sqrt{ghS}$, where g is gravity and S is slope, and Froude number $Fr = U/(gh)^{1/2}$. Based on the measurement precision of stream gauge readings, errors of 6–11 percent could be expected for mean hydraulic depths (relative errors are variable due to different depths), with
 195 a median of ± 7.6 percent. Accounting for the propagation of error from discharge and gauge readings, we estimate that the ratio U/U^* has a median error of ± 11.5 percent, with a maximum of ± 15 percent for the shallowest depths. A summary of reach-averaged hydraulic data is presented in Table 2.

To obtain an estimate of k_s using the hydraulic data, we used a Colebrook-White type formula ($k_{s,CW}^*$) neglecting the second term within the logarithm that applies to smooth-bed flows

$$200 \quad \frac{1}{\sqrt{f}} = K_1 \log \left(\frac{k_s}{K_2 h} + \frac{K_3}{4Re\sqrt{f}} \right) \quad (1)$$

~ where $K_1 = 2.03$, $K_2 = 11.09$, and $K_3 = 3.41$ as determined by Keulegan (1938), Re is the Reynolds number, and the Darcy-Weisbach friction factor f may be calculated from measured quantities using

$$205 \quad \sqrt{\frac{f}{8}} = \frac{\sqrt{ghS}}{U} \quad (2)$$

The channel thalweg for each DEM was determined by first locating pool centroids using the lowest ten percent of elevations at each cross-section, and then using Gaussian kernel regression to smooth vertices between the centroids. An example of the estimated thalweg location is shown in Figure 3. For each DEM, ten wetted cross-sections were reconstructed using the water surface elevation data, which were used to estimate reach-averaged hydraulics. Mean hydraulic depth was calculated as
 210 $h = A/w$, where A is cross-sectional area and w is the wetted width. Velocity was estimated using the continuity equation $U = Q/A$. Shear velocity is $U^* = \sqrt{ghS}$, where g is gravity and S is slope, and Froude number $Fr = U/(gh)^{1/2}$. A summary of this data is presented in Table 2.

3.1.3 Additional experiments

In addition to the experiments conducted for this study, we obtained topographic and hydraulic data for 86 step-pool experiments published by Hohermuth and Weitbrecht (2018). The experiments were conducted in a 1:20 Froude-scaled model
 215 of a mountain stream, utilizing a range of bed slopes (8–11–8–11 percent), channel widths (45–35 cm–0.15–0.35 m), and

Table 2. Summary of A-BES experimental data collected during the final portion of each experimental phase. Values represent the mean of the last five measurements. Re^* was calculated with $k = k_{s, pred}^* k = D_{84}$. The roughness length $k_{s, pred}^*$ is defined in Section 3.2. Units: W [m], Q [L/s], h [m], U [m/s], U^* [m/s], σ_z [m], k_s^* [m].

Exp	W	Q	h	F_r	U	U^*	$U/U^* - \sigma_z$	h/D_{84}	h/σ_z	Re^*	$k_{s, pred}^*$
Exp1a	0.30	1.50	0.014-0.015	0.95-0.96	0.36	0.053	6.76-0.0057	2.53-4.09	136-2.56	0.0034-600	4.32-0.0
Exp1b	0.30	1.00	0.012	0.85-0.86	0.29-0.30	0.049	6.00-0.0056	2.17-3.40	120-2.19	0.0032-528	3.72-0.0
Exp1c(1)	0.30	0.67	0.012	0.59-0.61	0.20-0.21	0.048	4.17-0.0051	3.26	2.27	105-460	0.0029-0
Exp1c(2)	0.30	1.00	0.013-0.014	0.70-0.73	0.25-0.26	0.051	4.96-0.0067	3.79	2.02	152-671	0.0039-0
Exp1c(3)	0.30	1.50	0.014	0.90-1.03	0.33-0.38	0.052	6.40-0.0063	3.94	2.24	154-678	0.0039-0
Exp1c(4)	0.30	2.25	0.018	1.03	0.43-0.44	0.060	7.28-0.0033	5.13	5.49	86-380	0.0019-0
Exp2a	0.08	0.40	0.015	0.92-0.94	0.35-0.36	0.054	6.47-0.0025	6.94-4.19	73-6.98	0.0018-323	11.550-0
Exp2b	0.08	0.27	0.013	0.75-0.74	0.26-0.27	0.050-0.051	5.29-0.0019	6.96-3.76	76-7.25	0.0020-343	7.340-0.0

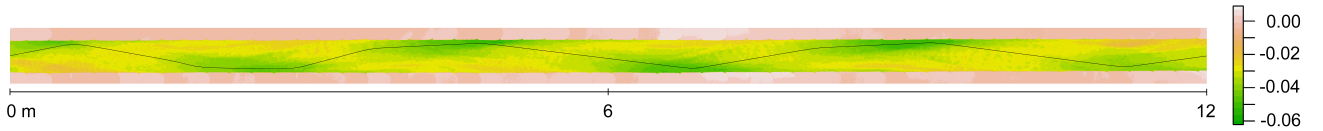


Figure 3. DEM of the pool-bar-riffle channel morphology at the end of Experiment 1a, with estimated position of the thalweg. Zero represents the downstream extent of the model.

discharges, unit discharges (0.019–0.167 m²/s). Four different grain size distributions were used, where D_{50} varied from 2.1–7.0 mm, and D_{90} remained around 58 mm. For a given experiment, a range of potentially usable elevation profiles were identified based on criteria for erroneous values, then the profile closest to the channel centreline was selected. Of the 86 experiments conducted, 83 experiments are used in this study. Thus, there is a total of 247 DEMs with associated hydraulic data when combined with the A-BES experiments.

3.2 The transform-roughness correlation approach

Here we specifically tailor-tailored the TRC approach to the geometric and hydraulic characteristics of gravel-bed channels. First, a MODWT is-was applied to the raw thalweg elevation profiles of each DEM, yielding a set of simplified profiles representing topographic variation occurring at different wavelengths. Second, we selected a roughness correlation for-irregular surfaces-developed by Forooghi et al. (2017) that predicts k_s from surface geometry in the fully rough regime-is, which was applied to each wavelength-to estimate the associated drag. Using direct numerical simulation (DNS). The relation was developed by conducting 38 direct numerical simulations in closed channels with systematically-generated surface geometries, an array

of systematically varied roughness geometries, both regular and irregular. By correlating surface and flow properties, Forooghi et al. (2017) proposed the following empirical relation

$$\frac{k_s}{k} \frac{k_s}{k_{ref}} = F(Sk, \Delta) \cdot F(ES) \quad (3)$$

where k is a measure of roughness peak heights $k_{ref} = 4.4\sigma_z$, and Sk is the skewness of the probability distribution of elevations. The functions $F(Sk, \Delta)$, $F(Sk)$, and $F(ES)$ are defined, respectively, as

$$F(Sk, \Delta) = \begin{cases} F(Sk), & \Delta \geq 0.35 \\ F(Sk)(1 + m(Sk) \cdot (\Delta - \Delta_0)), & \Delta \leq 0.35 \end{cases} \quad (4)$$

$$F(Sk) = 0.67Sk^2 + 0.93Sk + 1.3 \quad (5)$$

and

$$F(ES) = 1.05 \cdot (1 - e^{-3.8 \cdot ES}) \quad (6)$$

where Δ is a measure of the diversity of roughness peak heights (variability in the elevation of the peaks of roughness elements (height range divided by the mean, $\Delta = 0$ if peak heights are identical), $\Delta_0 = 0.35$ (not related to the critical ES value introduced below), and $m(Sk) = 1.47Sk^2 - 1.35Sk - 0.66$. The parameter ES is the effective slope which may be interpreted as the mean gradient of the local roughness elements (Napoli et al., 2008), and is given by

$$ES = \frac{1}{L} \int_L \left| \frac{dz(x)}{dx} \right| dx \quad (7)$$

where $z(x)$ is the height array, x is the streamwise direction, and L is the surface length in x . Effective slope is approximately proportional to drag in may be interpreted as the mean gradient of the local roughness elements (Napoli et al., 2008), and therefore represents the aspect-ratio of roughness elements rather than their vertical height. With other surface parameters kept equal, the roughness length is strongly dependent on ES within the range $0 < ES < 0.35$ (Napoli et al., 2008; Schultz and Flack, 2009). In the TRC approach, calculating the We calculated values of Δ parameter is impractical given that longer topographic wavelengths may for each wavelength by identifying peaks of the oscillations, and found $\Delta > 1$ for almost all cases. Values of Δ could not be estimated for the longest few wavelengths as they typically contain very few (or even one) complete oscillations that could be interpreted as roughness peaks. As a result, we simply use used the $F(Sk)$ term in Equation 4, which is likely appropriate given that for most natural surfaces $\Delta \gg 0$ (Forooghi et al., 2017). In the original equation, k was

defined as the peak-to-trough height of the surfaces, however, we adopt the standard deviation of elevations σ_z for the natural surfaces analysed herein as they are more topographically variable than the numerically-generated surfaces, and there is less bias towards extreme peaks and troughs. The effects of different choices of k are briefly explored in Figure ???. The estimated drag for each wavelength is expressed as $k_{s,RC}$. The roughness length for each wavelength is expressed as $k_{s,RC}$.

In addition to applying the roughness correlation to each wavelength, we applied it to each thalweg elevation profile to obtain an estimate of k_s . The, expressed as $k_{s,RC}^*$. Each profile was first detrended using the least-squares approach, which is not necessary with the wavelet transform as the overall trend is represented by a single wavelength and removed from all others. The experimental data and code that performs the MODWT and applies the roughness correlation is available online. In the following section, we present the results of the TRC approach applied to the experiments.

4 Results and Discussion

In this section, we primarily first seek to validate the TRC approach, and then focus on the results from multiscale roughness-length decomposition of Experiment 1a, which features a well-developed pool-riffle-bar-pool-bar-riffle sequence formed at a bank-full flow. First, we compare the topographic- and hydraulic-based estimates of k_s . Second, we demonstrate the relationship between estimates of k_s with and without the wavelet transform. Third, we show how the key parameters of the roughness correlation (effective slope and standard deviation, standard deviation, effective slope, skewness) vary across each wavelength. Second/Fourth, we estimate the relative contribution of different scales of bed topography to the total drag-roughness length and explain how the estimated values relate to the key parameters and the characteristics of the experimental surfaces. Third, we perform a sensitivity analysis for the choice of analysing function (known as the ‘mother wavelet’) in experiments. Fifth, we compare the performance of different roughness lengths in estimating flow resistance. Finally, we discuss the significance, limitations, and potential applications of the TRC approach.

4.1 Estimates of total k_s

The relationship between the estimates of k_s from the MODWT and the choice of k in the roughness correlation. Finally, using all of the available experiments, we demonstrate that $k_{s,RC}^*$ and the Colebrook-White equation $k_{s,CW}^*$ varies across the three different channel morphologies (Figure 4). Here, we consider $k_{s,CW}^*$ to be a ‘measured’ quantity which the roughness correlation may be used to estimate total flow resistance using a conventional equation. tested against. The pool-bar-riffle experiments ($W = 0.3$ m) have the closest relationship between the two k_s estimates, with the distribution centering along the 1:1 line (median $k_{s,CW}^*/k_{s,RC}^* = 0.99$). The close relationship between the two independent estimates of k_s supports the one-dimensional approach for these experiments as it indicates that the single elevation profile captures the roughness elements that contribute the greatest resistance to flow. Also, the results supports the application of the Forooghi et al. (2017) roughness correlation to the A-BES experiments, which have more complex surface characteristics and far lower values of relative submergence compared to the numerical domain within which the correlation was developed.

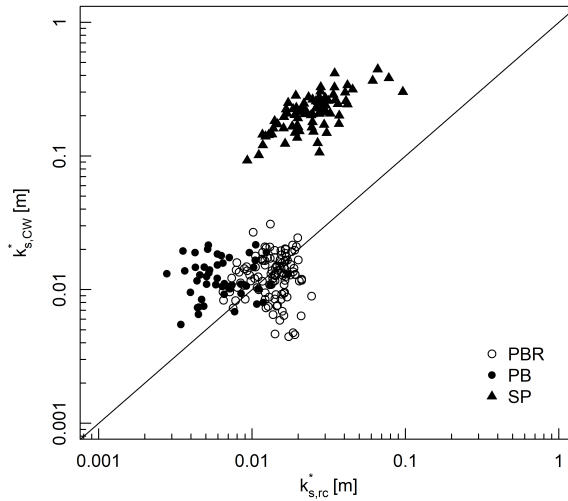


Figure 4. Relationship between total k_s estimated by the Forooghi et al. (2017) roughness correlation (Equation 3) and the Colebrook-White approach (Equation 1). Data for the A-BES experiments are grouped by channel morphology (Table 1), and the Hohermuth and Weitbrecht (2018) step-pool (SP) experiments are included.

Figure ?? shows the effective slope of each topographic wavelength (or spatial scale) over the course of Experiment 1a. The effective slope is greatest at the grain-scale wavelengths ($\lambda \leq D_{max}$) where the surface is locally rough and reduces as the wavelength increases and. The distribution of plane-bed experiments ($W = 0.08$ m) overlap with the 1:1 line, although there is a consistent under-prediction of k_s using the roughness correlation by a factor-of-two (median $k_{s,cw}^*/k_{s,rc}^* = 1.84$). In the case of the step-pool experiments, there is a significant under-prediction of k_s by the roughness correlation of around an order-of-magnitude (median $k_{s,cw}^*/k_{s,rc}^* = 9.11$), which may be explained by the lower relative submergence (median $h/D_{84} = 1.48$).

The next stage in validating the TRC approach is comparing the values of $k_{s,rc}^*$ and $\Sigma k_{s,rc}$, whereby the latter is the estimate provided by applying the roughness correlation to each wavelength (giving values of $k_{s,rc}$), and then taking the sum. In other words, this is comparing the values of k_s estimated by the roughness correlation with and without the wavelet transform as an intermediate stage. This comparison is important for two reasons. First, the topography is more locally subdued. This is demonstrated in Figure 1b, where wavelengths at the grain scale have more acute oscillations than those at longer wavelengths. The main exception to this trend is the wavelength of around TRC approach is an extension of the linear superposition approach, which assumes that the hydraulic effect of adding up different roughness elements is approximately linear (Millar, 1999; Wilcox and Wohl, 2006; Rickenmann and Recking, 2011). In practice, superimposing roughness elements

300 may have non-linear feedback effects (Yen, 2002; Li, 2009; Wilcox and Wohl, 2006), such that $k_{s,rc}^*$ and $\Sigma k_{s,rc}$ may potentially not be correlated.

Second, values of $k_{s,rc}^*$ and $\Sigma k_{s,rc}$ may differ as the process of signal decomposition and recombination is characterised by wave interference. For example, for each thalweg elevation profile there are two estimates of amplitude (1) the standard deviation of elevations σ_z , and (2) ~~where there is a prominent peak in the ES distribution, associated with the development of~~ $\Sigma \sigma_\lambda$, which is the pool-riffle-bar sequence approximately ten minutes into the experiment. It is important to note that most of the topographic wavelengths have values of ES (sum of σ_z for each wavelength. However, due to positive and negative wave interference σ_z and k_s/k in Equation 3) that are smaller than the surfaces used by Forooghi et al. (2017) to develop the roughness correlation. Thus, it may be more appropriate to focus on the relative values of $k_{s,pred}$ for a specific combination of channel geometry $\Sigma \sigma_\lambda$ may significantly differ. Decomposing and recombining wavelengths alters the position and magnitude of peaks and troughs in the wavelengths, and therefore, their amplitude. Thus, wave interference may potentially confound estimates of k_s if a transform is used. For the above two reasons, it is important to demonstrate that values of $k_{s,rc}^*$ and roughness correlation $\Sigma k_{s,rc}$ are correlated, even if they are unlikely to be the same.

The transform and non-transform estimates of k_s are positively correlated with an approximately linear relationship (Figure 5). It is worth noting that the two datasets are characterised by different slopes and intercepts, which may be explained by the specific characteristics of each topographic dataset (e.g. geometry, resolution) giving rise to different patterns of wave interference. However, it appears that nonlinear superposition effects and wave interference do not invalidate the TRC approach for these datasets.

Figure 6a shows

4.2 Application of TRC approach

In Experiment 1a there is a general increase in the standard deviation of each topographic wavelength for Experiment 1a. Except for elevations with increasing wavelength (Figure 6a). Over the first ten minutes (i.e. first two DEMs) during which the bed morphology is developing the first two elevation profiles), there is a minor peak an increase in σ_z at the scale of 3 cm, and a major peak at the scale of above $\lambda > 0.5$ m, with the greatest increase at $\lambda \approx 2$ m, but smaller wavelengths remain largely unchanged. At the smallest scales, topographic variation wavelengths, the σ_z tends towards zero, and there is some contribution to σ_z at the largest scale wavelengths due to the slightly concave or convex shape of the profile, evident in Figure 1a. Figure 6b presents this data the value of σ_z for each wavelength as a cumulative percentage, which shows that the grain scale accounts. This type of graph is similar to the Form Size Distribution (FSD) proposed by Nyander et al. (2003), which was the cumulative variance of each wavelength calculated using a 2D DWT. For comparison, we provide the bulk grain size distribution within the same space (where wavelength is grain diameter). Grain-scale wavelengths account for less than five percent of all topographic variation. This figure is the same as the Form Size Distribution (FSD) proposed by Nyander et al. (2003), given that the arrangement of grains contribute to bed structures that usually exceed the amplitude of individual grains.

The effective slope is greatest at the grain scale wavelengths ($\lambda < D_{max}$) where the surface is characterized by closely-bunched peaks and troughs associated with individual grains (Figure 7b). Values of ES decrease with increasing λ , due to the presence

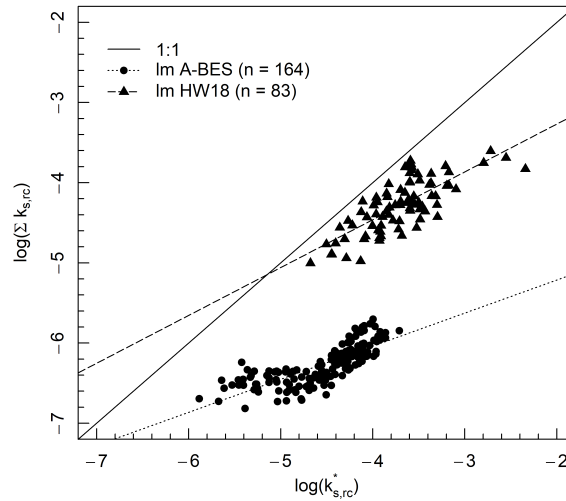


Figure 5. Effective slope of each topographic wavelength during Experiment 1a, where each line represents a point in time. Vertical dashed line represents Relationship between $k_{s,rc}^*$ and $\Sigma k_{s,rc}$ for the largest grain diameter in the experiment A-BES and Hohermuth and Weitbrecht (2018) experiments. The shaded area represents the range of ES values of the surfaces generated by Forooghi et al. (2017).

of more gently undulating roughness elements. This is evident in the example (Figure 1c), where the 4 mm wavelength has high ES indicated by sharp oscillations (but low σ_z), and the 2 m wavelength has low ES (but high σ_z). The main exception to the downwards trend of ES with increasing λ is the wavelength of around 2 m where there is a prominent peak in the ES distribution, associated with the development of the pool-riffle-bar sequence approximately ten minutes into the experiment. Note that most of the topographic wavelengths have values of ES (and k_s/k in Equation 3) that are smaller than the surfaces used by Forooghi et al. (2017) to develop the roughness correlation. Wavelengths tend to be positively skewed at small and large scales, with a negatively-skewed region between $0.1 > \lambda > 1.0$ m (Figure 7a). There is little change in the pattern of skewness over the course of the experiment.

Using the TRC approach, we present the distribution of k_s predicted. The distribution of $k_{s,rc}$ values predicted for each wavelength using Equation 3 is presented in Figure 8a. Following the format of ‘grain size distribution’ and ‘form size distribution’, we term this style of plot the drag size distribution (DSD). There is a major peak in the DSD at the scale of $\lambda \approx 2$ m and (the spacing of pools, bars, and riffles), and a minor peak at the scale of approximately 5 mm $\lambda \approx 0.005$ m (around the size of the largest grains). At small scales/wavelengths, and large scales/wavelengths especially, estimated k_s tends downwards. Figure 8b presents the DSD as a cumulative percentage, which shows that the k_s associated with the grain scale is estimated to account for approximately 30 percent of the total k_s . This proportion of grain- and form-drag is similar to estimates in gravel-

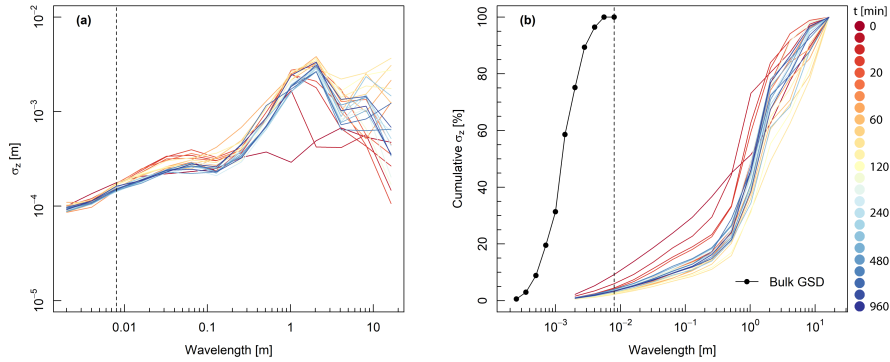


Figure 6. Form size distribution during Experiment 1a, where each line represents a point in time, and the initial screeded bed is included. The standard deviation of each topographic wavelength is presented as an (a) absolute, and (b) cumulative percentage, for each thalweg elevation profile. The bulk grain size distribution is included, where the wavelength corresponds to grain diameter. The vertical dashed line represents the largest grain diameter in the experiment.

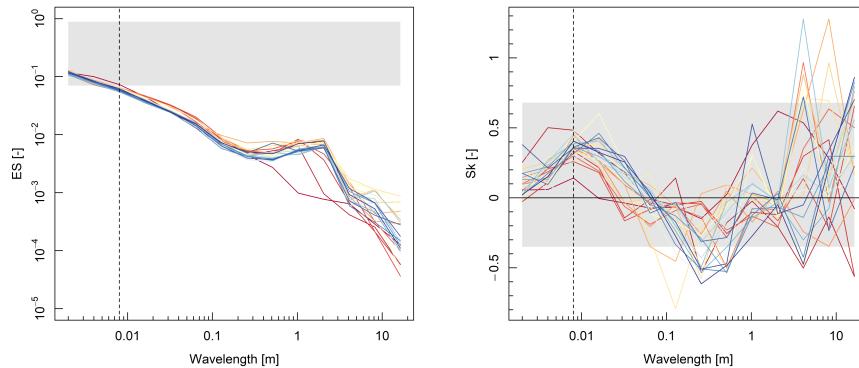


Figure 7. Form size distribution during Experiment 1a. Standard deviation of each topographic wavelength presented as an (a) absolute Effective slope and (b) cumulative percentage, for longitudinal profiles skewness of each topographic wavelength during Experiment 1a. The shaded area represents the experiment range of ES and Sk values of the surfaces generated by Forooghi et al. (2017). Refer to Figure ??-6 for legend.

bed rivers with similar morphologies (Hey, 1988; Parker and Peterson, 1980; Prestegard, 1983), which further indicates that the TRC approach provides physically realistic estimates of drag a physically realistic decomposition of the roughness length.

350 Figure ?? demonstrates the dependency of $\sum k_{s,pred}$ (i.e. sum of $k_{s,pred}$ for a given DEM) on the choice of mother wavelet and the k value in the roughness correlation. Various mother wavelets from the Daubechies family have been used when

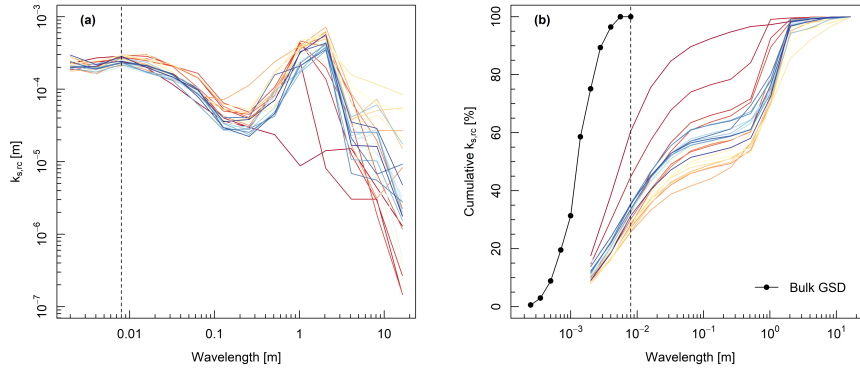


Figure 8. Drag size distribution during over the course of Experiment 1a. Estimated drag associated with The estimated roughness length of each topographic wavelength presented as an (a) absolute, and (b) cumulative percentage, for longitudinal profiles during the experiment. Refer to Figure ??-6 for legend. Note that the absolute values of $k_{s, pred}$ appear unusually small for the surfaces ($\ll 1$ mm) compared to values of σ_z , which is discussed later.

applying wavelet transform to river bed topography (Nyander et al., 2003; Gutierrez et al., 2013; Qin et al., 2015), and for the same k value, these mother wavelets yield similar results. The values of $\Sigma k_{s, pred}$ are more sensitive to the choice of k . If standard deviation is used as the estimate of k , whilst changing Ψ , there is a relatively similar pattern of $\Sigma k_{s, pred}$. If the absolute range of elevations is used as k , as was used by (Forooghi et al., 2017), extreme outliers in the elevation profile disrupt a physically realistic pattern of total drag across the experiments, which should consist of at least an initial increase as the pool-bar-riffle sequence emerges.

Sensitivity analysis of $\Sigma k_{s, pred}$ to choice of mother wavelet Ψ in MODWT and k in the roughness correlation for Experiment 1a, where $z_{max} - z_{min}$ is the maximum range of elevations. The combination of σ_z and Daubechies 4 wavelet is used in this study.

The approach of adding up the effect of different roughness elements to estimate a net effect, although established in the literature (Cowan, 1956; Einstein and Banks, 1950; Hey, 1988; Leopold et al., 1960; Millar, 1999), has been demonstrated to have limitations given that superimposed combinations of different roughness elements may produce drag feedbacks in either direction (Li, 2009; Wilcox and Wohl, 2006). Thus, it is important to demonstrate that $\Sigma k_{s, pred}$ is proportional to the total k_s . In Figure 9 we compare the performance of geometric (D_{84} , σ_z) and hydraulic ($k_{s, rc}^*$, $k_{s, CW}^*$) estimates of roughness length in estimating flow resistance, using the Ferguson (2007) variable-power equation (VPE, Appendix A). We provide two fitted relations for the VPE that provide baselines for comparison; (1) coefficients determined by a systematic review of σ_z as a roughness measure (Chen et al., 2020), and (2) $k_{s, CW}^*$ values which are back-calculated from the hydraulic measurements. Given that these two relations represent geometric and hydraulic approaches to estimating roughness, they describe significantly different relationships between the friction factor and relative submergence.

Using data from all experiments conducted for this study, in addition to the ~~There is a weak relationship between f and h/k if k is estimated by the bulk D_{84} values (as an approximation of the surface GSD). Using σ_z as an estimate of k the step-pool experiments of Hohermuth and Weitbrecht (2018), Figure 5 compares the relationship between $\Sigma k_{s,pred}$ and experiments are consistent with the VPE relation provided by Chen et al. (2020), but σ_z overestimates k in the $k_{s,pred}^*$, the latter being the estimate of A-BES experiments. Using values of k_s obtained by applying the roughness correlation to the elevation profile without the transform. Each of from the two datasets are described by a linear relationship, which demonstrates that both the transform and non-transform estimates of k_s are proportional. This validates the TRC approach for a given dataset, however, it is worth noting that the two datasets are characterised by different slopes. The difference in slope likely arises due to the specific characteristics of each topographic dataset, which affect the wavelet decomposition of the wavelengths, and in turn, the values of $k_{s,pred}$. The choice of k in the roughness correlation does not affect the linear relationship between $k_{s,pred}^*$ and $\Sigma k_{s,pred}$.~~

Relationship between $k_{s,pred}^*$ and $\Sigma k_{s,pred}$ for the pool-riffle (PR) experiments carried out for this study, as well as the step-pool (SP) experiments conducted by Hohermuth and Weitbrecht (2018):

Figure 9 compares the relationship between estimated flow resistance $(8/f)^{1/2}$ and relative submergence h/k , using two different values of k . In Figure 9a, relative submergence is calculated using σ_z , which is now common in gravel-bed rivers, whereas in Figure 9b, it is calculated using $k_{s,pred}^*$. Ferguson's (2007) variable-power equation (Appendix A) is applied with coefficients reported by Chen et al. (2020), which were fitted to a wide range of gravel-bed channels using $k = \sigma_z$. It is interesting to note that the $k_{s,pred}^*$ approach to relative submergence yields a closer fit to the Chen relation, quantified by a 30-percent smaller root-mean-square error. This result suggests that, the values of relative submergence for the A-BES experiments are consistent with the Colebrook-White relation, but there is an underprediction of k_s in the step-pool experiments. These results suggest that estimates of k_s based on Equation 3 are useful in predicting from roughness correlations may contribute to improved estimates of flow resistance in rivers, and thus provides evidence for the multiscale drag decompositions some conditions. The results also affirm that roughness metrics derived from surface topography are superior to ones derived from the grain size distribution.

395 5 Implications for flow resistance in rivers, applications, and limitations

The roughness correlation developed by Forooghi et al. (2017) incorporates Recently proposed roughness correlations in fluid dynamics (e.g. Forooghi et al., 2017; De Marchis et al., 2020) incorporate information regarding both the height of the roughness elements (a vertical roughness scale, Nikora et al. 1998 e.g. σ_z) and the arrangement or spacing of roughness elements (a horizontal roughness scale, Bertin and Friedrich 2014 e.g. ES). In isolation, either one of these roughness scales may be misleading. For example, effective slope is a horizontal roughness metric and can be proportional to drag for some surfaces (Napoli et al., 2008; Schultz and Flack, 2009). Thus, in isolation, Figure ?? would indicate that the small-scale bed features are most effective at producing drag. Alternatively, the standard deviation of surface elevations is a vertical roughness metric and has also shown to be proportional to flow resistance (Aberle et al., 1999; Chen et al., 2020). Therefore, in isolation, Figure

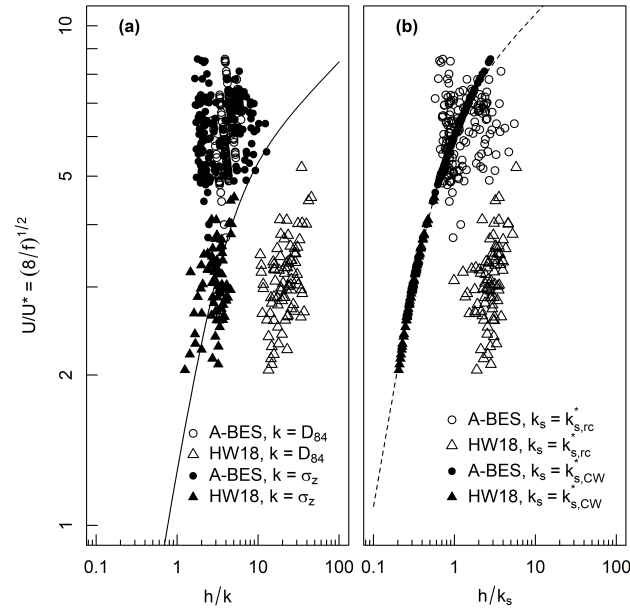


Figure 9. Plot of $(8/f)^{1/2}$ against relative submergence h/k for A-BES and Hohermuth and Weitbrecht (2018) data, where using four different roughness lengths (a) $k = \sigma_z D_{84}$, and (b) $k = \sigma_z k_{s,rc}^*$, $k = \sigma_z k_{s,CW}^*$. Solid The solid line is the Ferguson (2007) variable-power equation (VPE) using coefficients $a_1 = 5.77$ – 3.94 and $a_2 = 1.24$ – 1.36 determined by a systematic review of σ_z as a roughness measure (Chen et al., 2020). Root-mean-square errors are 2.03 and 1.42, respectively. Dashed The dashed line is the VPE fitted to the $h/k_{s,CW}^*$ data, where yielding coefficients of $a_1 = 4.81$ – 7.22 and $a_2 = 2.36$ (note: VPE could not be fitted to h/σ_z) 11.19.

6 could lead to the interpretation that only the largest scale bed features produce drag, metrics may contribute to an incomplete – and potentially misleading – estimate of flow resistance. It is important to recognize that recognise that, depending on the surface of interest, drag the total roughness length is usually a compromise between vertical and horizontal roughness, which is inherent in Equation 3 and the drag size distribution (Figure 8) scales of the bed surface.

In gravel-bed rivers, which are typically ungauged, and where measurement of hydraulic variables is subject to practical limitations (Miller, 1958), flow resistance is typically usually estimated using only a vertical roughness scale. Upon introducing his method of sampling coarse bed material, Wolman (1954) remarked that these data could be used to estimate hydraulic roughness, and Lane (1957) agreed, based on the notion that grain diameter represents a vertical roughness scale as demonstrated by Nikuradse (1933) such as grain diameter (Hey, 1979; Ferguson, 2007). However, the relationship between grain diameter and flow resistance breaks down in natural channels for two main reasons (see Adams, 2020a): (1) grain diameter does not account for larger and often more hydrodynamically significant roughness elements (Sundborg, 1956; Leopold et al., 1964; Bath 415 dissipative roughness elements, and (2) it does not consider the horizontal spacing of these larger roughness elements (Schlichting, 1936; No, which has a systematic effect on drag (Morris, 1955; Leonardi et al., 2007; Napoli et al., 2008).

hydraulics. In recent years, the increased availability of high-resolution topographic data has led to the adoption of σ_z as a roughness scale metric in gravel-bed rivers, on the basis that it ~~accounts for~~ includes information regarding larger-scale bed structures (Aberle et al., 1999; Aberle and Smart, 2003; Cadol and Wohl, 2013; Smart et al., 2002; Yochum et al., 2014)(Chen et al., 2020). However, σ_z only improves upon the first deficiency of grain-based roughness metrics ~~;~~ and, consequently, it ~~cannot be considered a measure of hydraulic roughness~~ has inherent limitations. The roughness correlation ~~used herein may be a significant improvement over~~ presented by Forooghi et al. (2017) may improve upon existing roughness metrics ~~as it incorporates both vertical and horizontal roughness scales,~~ used in gravel-bed rivers, and it may be applied to most datasets where σ_z is calculated.

425 The TRC analysis has direct applications across geomorphology. Quantification of scale-dependent patterns of channel topography and roughness length may contribute to form- and ~~provides a direct semi-empirical estimate~~ process-based classifications of channel morphology and dynamics. There have been numerous attempts to classify channels based on in-channel features and their associated processes (e.g. Montgomery and Buffington, 1997), however, analysis of bed topography is typically qualitative. We expect that different channel types exhibit distinctive scale-based patterns of σ_z and k_s , which would enable a
430 quantitative and heuristic classification index.

The scale-based decomposition of k_s may assist in identifying and forecasting the hydraulic influence of specific roughness elements in channels. For example, through the manipulation of spatial datasets by the addition or removal of features, the role of natural in-channel features (e.g. large wood) and engineering designs (e.g. rock chutes) could be isolated and determined for flood conditions. Also, multiscale roughness length decomposition may contribute to an understanding of bedload transport
435 processes, where the partitioning of bed stresses between grain and form scales is essential in making accurate predictions (Ancy, 2020). ~~Moreover, roughness correlations of this variety can be applied to most datasets where σ_z is calculated.~~

However, in its current form, there are some conditions in which the TRC approach is limited. The discrepancy between topographic and hydraulic estimates of k_s for step-pool channels highlights the potential limitations of the roughness correlation in steep gravel-bed rivers where slope and relative submergence have a greater hydraulic influence. In channels with significant
440 planform resistance, the approach may require modification to account for the slope and curvature of the channel. In multi-thread channels, several profiles may need to be employed, and the results weighted according to the size of the channel. Even under such conditions, the basic multiscale roughness length decomposition may still have considerable value with appropriate research questions.

6 Conclusions

445 The transform-roughness correlation approach ~~allows researchers to estimate~~ estimates the relative contribution of various scales of bed-in-channel topography to the total drag roughness length. By modifying the roughness correlation to suit the hydraulic conditions, multiscale drag roughness length decomposition may be achieved in virtually any type of river or numerical model, and perhaps boundary-layers in other environments. The only requirement is that the topographic data is of a sufficient resolution and spatial extent to capture the scales over which the hydraulically-significant roughness elements occur, and data

450 of this quality is only becoming more available to geomorphologists ~~over time~~. In particular, we expect that given the continual advances in methods for collecting bathymetric data in both shallow (Kasvi et al., 2019) and deep channels (Dietrich, 2017), applying the TRC approach will become increasingly practical in natural rivers.

Given that the TRC approach ~~may provide new and more~~ provides novel and detailed information regarding the ~~effect of bed geometry on~~ interaction between surface topography and fluid dynamics, ~~incorporating both horizontal and vertical scales of~~ roughness, it may contribute to advances in hydraulics ~~as well as an understanding of channel morphodynamics. The estimates of total~~ channel morphodynamics, and bedload transport. Estimates of k_s from semi-empirical roughness correlations may ~~present~~ provide more immediate benefits by ~~servicing as replacements for~~ improving upon representative roughness values ; ~~which have historically been necessitated by technological limitations.~~

~~The application of the TRC approach herein demonstrates the limitations of commonly used approaches to~~ in estimating flow resistance ~~in rivers, which rely solely on representations of vertical roughness and ignore their horizontal arrangement. Also, it highlights the utility of wavelet transform as a tool that provides intuitive representations of channel bed topography. The TRC approach is currently being used to explore channel morphodynamics and bedload transport using laboratory experiments. We are currently conducting experiments to further develop and apply these ideas.~~

Code and data availability. Data and code are available online (<https://doi.org/10.5281/zenodo.4016397>; Adams (2020b)).

465 **Appendix A: Ferguson (2007) variable-power equation**

Ferguson (2007) presented the variable-power flow resistance equation

$$(8/f)^{1/2} = \frac{a_1 a_2 (h/k)}{(a_1^2 + a_2^2 (h/k)^{5/3})^{1/2}} \quad (\text{A1})$$

where a_1 and a_2 are empirically-derived coefficients, h is flow depth or hydraulic radius, and k is ~~some representative roughness scale~~ a representative roughness length.

470 *Author contributions.* DLA is responsible for conceptualization, investigation, formal analysis, and writing. AZ provided expertise in open-channel flow, contributing to the interpretation and communication of the results and the proposed technique.

Competing interests. The authors declare that they have no conflict of interest.

Acknowledgements. The authors would like to thank William Booker, Lucy MacKenzie, Brett Eaton, and Ian Rutherford for reviewing the original manuscript, and Benjamin Hohermuth for providing the laboratory step-pool data. This work was supported by postgraduate
475 scholarships provided to DLA by the Australian and Canadian Governments.

References

- Aberle, J. E. and Smart, G. M.: The influence of roughness structure on flow resistance on steep slopes, *Journal of Hydraulic Research*, 41, 259–269, 2003.
- Aberle, J. E., Dittrich, A., and Nestmann, F.: Description of steep stream roughness with the standard deviation s , in: Proceedings of the 28th
480 Congress of the IAHR, Graz, Austria, 1999.
- Adams, D. L.: Toward bed state morphodynamics in gravel-bed rivers, *Progress in Physical Geography*,
<https://doi.org/10.1177/0309133320900924>, 2020a.
- Adams, D. L.: Code and example data for transform-roughness correlation (TRC) approach, <https://doi.org/doi.org/10.5281/zenodo.4016397>,
2020b.
- 485 Addison, P. S.: Introduction to redundancy rules: the continuous wavelet transform comes of age, *Philosophical Transactions of the Royal Society A: Mathematical, Physical and Engineering Sciences*, 376, 1–15, <https://doi.org/10.1098/rsta.2017.0258>, 2018.
- Ancey, C.: Bedload transport: a walk between randomness and determinism. Part 2. Challenges and prospects, *Journal of Hydraulic Research*,
58, 18–33, <https://doi.org/10.1080/00221686.2019.1702595>, 2020.
- Ashworth, P. J. and Ferguson, R. I.: Size-selective entrainment of bed-load in gravel bed streams, *Water Resources Research*, 25, 627–634,
490 <https://doi.org/10.1029/WR025i004p00627>, 1989.
- Bathurst, J. C.: Flow resistance in boulder-bed streams, in: *Gravel-bed rivers*, edited by Hey, R. D., Bathurst, J. C., and Thorne, C. R., pp.
443–465, John Wiley & Sons, Chichester, U.K., 1982.
- Bergeron, N. E.: Scale-space analysis of stream-bed roughness in coarse gravel-bed streams, *Mathematical Geology*, 28, 537–561,
<https://doi.org/10.1007/BF02066100>, 1996.
- 495 Bertin, S. and Friedrich, H.: Measurement of Gravel-Bed Topography: Evaluation Study Applying Statistical Roughness Analysis, *Journal of Hydraulic Engineering*, 140, 269–279, [https://doi.org/10.1061/\(ASCE\)HY.1943-7900.0000823](https://doi.org/10.1061/(ASCE)HY.1943-7900.0000823), <http://ascelibrary.org/doi/10.1061/{%}28ASCE{%}29HY.1943-7900.0000823>, 2014.
- Bray, D. I.: Flow resistance in gravel bed rivers, in: *Gravel-bed rivers*, edited by Hey, R. D., Bathurst, J. C., and Thorne, C. R., pp. 109–133,
John Wiley & Sons, Chichester, U.K., 1982.
- 500 Buffington, J. M. and Montgomery, D. R.: A systematic analysis of eight decades of incipient motion studies, with special reference to
gravel-bedded rivers, *Water Resources Research*, 33, 1993–2029, <https://doi.org/10.1029/97WR03138>, 1997.
- Cadol, D. and Wohl, E. E.: Variable contribution of wood to the hydraulic resistance of headwater tropical streams, *Water Resources Research*,
49, 4711–4723, <https://doi.org/10.1002/wrcr.20362>, 2013.
- Cameron, S. M., Nikora, V. I., and Stewart, M. T.: Very-large-scale motions in rough-bed open-channel flow, *Journal of Fluid Mechanics*,
505 814, 416–429, <https://doi.org/10.1017/jfm.2017.24>, 2017.
- Chen, X., Hassan, M. A., An, C., and Fu, X.: Rough correlations: Meta-analysis of roughness measures in gravel bed rivers, *Water Resources Research*, 2020.
- Chow, T. V.: *Open channel hydraulics*, McGraw-Hill Book Company, Inc, New York, 1959.
- Church, M. A.: *Rivers – Physical, Fluvial and Environmental Processes*, Springer, <https://doi.org/10.1007/978-3-319-17719-9>, <http://link.springer.com/10.1007/978-3-319-17719-9>, 2015.
- 510 Clifford, N. J., Robert, A., and Richards, K. S.: Estimation of flow resistance in gravel-bedded rivers: A physical explanation of the multiplier
of roughness length, *Earth Surface Processes and Landforms*, 17, 111–126, <https://doi.org/10.1002/esp.3290170202>, 1992.

- Cowan, W. L.: Estimating hydraulic roughness coefficients., *Agricultural Engineering*, 7, 473–475, 1956.
- Davies, T. R. H. and Sutherland, A. J.: Resistance to flow past deformable boundaries, *Earth Surface Processes*, 5, 175–179, 1980.
- 515 De Marchis, M., Saccone, D., Milici, B., and Napoli, E.: Large Eddy Simulations of Rough Turbulent Channel Flows Bounded by Irregular Roughness: Advances Toward a Universal Roughness Correlation, *Flow, Turbulence and Combustion*, 105, 627–648, <https://doi.org/10.1007/s10494-020-00167-5>, <https://doi.org/10.1007/s10494-020-00167-5>, 2020.
- Dietrich, J. T.: Bathymetric Structure-from-Motion: extracting shallow stream bathymetry from multi-view stereo photogrammetry, *Earth Surface Processes and Landforms*, 42, 355–364, <https://doi.org/10.1002/esp.4060>, <http://doi.wiley.com/10.1002/esp.4060>, 2017.
- 520 Eaton, B. C. and Church, M. A.: A graded stream response relation for bed load-dominated streams, *Journal of Geophysical Research*, 109, 1–18, <https://doi.org/10.1029/2003JF000062>, 2004.
- Eaton, B. C. and Church, M. A.: Channel stability in bed load-dominated streams with nonerodible banks: Inferences from experiments in a sinuous flume, *Journal of Geophysical Research: Earth Surface*, 114, 1–17, <https://doi.org/10.1029/2007JF000902>, 2009.
- Einstein, H. A. and Banks, R. B.: Fluid resistance of composite roughness, *Transactions of the American Geophysical Union*, 31, 603–610, 525 1950.
- Ferguson, R. I.: Flow resistance equations for gravel- and boulder-bed streams, *Water Resources Research*, 43, 1–12, <https://doi.org/10.1029/2006WR005422>, 2007.
- Field, J. P. and Pelletier, J. D.: Controls on the aerodynamic roughness length and the grain-size dependence of aeolian sediment transport, *Earth Surface Processes and Landforms*, 43, 2616–2626, <https://doi.org/10.1002/esp.4420>, 2018.
- 530 Forooghi, P., Stroh, A., Magagnato, F., Jakirlic, S., and Frohnapfel, B.: Towards a Universal Roughness Correlation, *Journal of Fluids Engineering*, 139, 1–12, <https://doi.org/10.1115/1.4037280>, 2017.
- Furbish, D. J.: Conditions for geometric similarity of coarse stream-bed roughness, *Mathematical Geology*, 19, 291–307, <https://doi.org/10.1007/BF00897840>, 1987.
- Griffiths, G. A.: Flow resistance in coarse gravel bed rivers, *Journal of the Hydraulics Division*, 107, 899–918, 1981.
- 535 Gutierrez, R. R., Abad, J. D., Parsons, D. R., and Best, J. L.: Discrimination of bed form scales using robust spline filters and wavelet transforms: Methods and application to synthetic signals and bed forms of the Río Paraná, Argentina, *Journal of Geophysical Research: Earth Surface*, 118, 1400–1419, <https://doi.org/10.1002/jgrf.20102>, 2013.
- Hey, R. D.: Flow Resistance in Gravel-Bed Rivers, *Journal of the Hydraulics Division*, 105, 365–379, 1979.
- Hey, R. D.: Bar Form Resistance in Gravel-Bed Rivers, *Journal of Hydraulic Engineering*, 114, 1498–1508, 1988.
- 540 Hohermuth, B. and Weitbrecht, V.: Influence of Bed-Load Transport on Flow Resistance of Step-Pool Channels, *Water Resources Research*, 54, 5567–5583, <https://doi.org/10.1029/2017WR021523>, 2018.
- Jimenez, J.: Turbulent Flows over Rough Walls, *Annual Review of Fluid Mechanics*, 36, 173–196, <https://doi.org/10.1146/annurev.fluid.36.050802.12210>, 2004.
- Kasvi, E., Salmela, J., Lotsari, E., Kumpula, T., and Lane, S. N.: Comparison of remote sensing based approaches for mapping bathymetry 545 of shallow, clear water rivers, *Geomorphology*, 333, 180–197, <https://doi.org/10.1016/j.geomorph.2019.02.017>, <https://doi.org/10.1016/j.geomorph.2019.02.017>, 2019.
- Keulegan, G. H.: Laws of turbulent flow in open channels, *Journal of Research of the National Bureau of Standards*, 21, 707, <https://doi.org/10.6028/jres.021.039>, 1938.
- Keylock, C. J., Singh, A., and Fofoula-Georgiou, E.: The complexity of gravel bed river topography examined with gradual wavelet reconstruction, *Journal of Geophysical Research: Earth Surface*, 119, 682–700, <https://doi.org/10.1002/2013JF002999>, 2014. 550

- Kumar, P. and Foufoula-Georgiou, E.: Wavelet Analysis for geophysical applications, *Reviews of Geophysics*, 34, 385–412, <https://doi.org/10.1029/97RG00427>, 1997.
- Lane, E. W.: A study of the shape of channels formed by natural streams flowing in erodible material, Tech. rep., MRD Sediment Series no. 9, United States Army Corps, Engineering Division, 1957.
- 555 Lee, A. J. and Ferguson, R. I.: Velocity and flow resistance in step-pool streams, *Geomorphology*, 46, 59–71, [https://doi.org/10.1016/S0169-555X\(02\)00054-5](https://doi.org/10.1016/S0169-555X(02)00054-5), 2002.
- Leonardi, S., Orlandi, P., and Antonia, R. A.: Properties of d- and k-type roughness in a turbulent channel flow, *Physics of Fluids*, 19, 1–6, <https://doi.org/10.1063/1.2821908>, 2007.
- Leopold, L. B., Bagnold, R. A., Wolman, M. G., and Bush, L. M.: Flow resistance in sinuous or irregular channels, Tech. rep., 1960.
- 560 Leopold, L. B., Wolman, M. G., and Miller, J. P.: *Fluvial processes in geomorphology*, Freeman, San Francisco, CA, 1964.
- Li, G.: Preliminary study of the interference of surface objects and rainfall in overland flow resistance, *Catena*, 78, 154–158, <https://doi.org/10.1016/j.catena.2009.03.010>, 2009.
- Limerinos, J. T.: Determination of the Manning Coefficient From Measured Bed Roughness in Natural Channels, Tech. rep., 1970.
- MacKenzie, L. G. and Eaton, B. C.: Large grains matter: contrasting bed stability and morphodynamics during two nearly identical experi-
565 ments, *Earth Surface Processes and Landforms*, 42, 1287–1295, <https://doi.org/10.1002/esp.4122>, 2017.
- Millar, R. G.: Grain and form resistance in gravel-bed rivers, *Journal of Hydraulic Research*, 37, 303–312, <https://doi.org/10.1080/00221686.1999.9628249>, 1999.
- Miller, J. P.: High mountain streams: Effects of geology on channel characteristics and bed material, *New Mexico State Bureau of Mines and Mine Resources Memoir 4*, p. 51 pp., 1958.
- 570 Montgomery, D. R. and Buffington, J. M.: Channel-reach morphology in mountain basins, *Geological Society of America Bulletin*, 109, 596–611, [https://doi.org/10.1130/0016-7606\(1997\)109<0596](https://doi.org/10.1130/0016-7606(1997)109<0596), 1997.
- Morris, H. M.: A new concept of flow in rough conduits, *Transactions of the American Society of Civil Engineers*, 120, 373–398, 1955.
- Nanson, G. C. and Huang, H. Q.: Least action principle, equilibrium states, iterative adjustment and the stability of alluvial channels, *Earth Surface Processes and Landforms*, 33, 923–942, <https://doi.org/10.1002/esp.1584>, <http://doi.wiley.com/10.1002/esp.1584>, 2008.
- 575 Nanson, G. C. and Huang, H. Q.: A philosophy of rivers: Equilibrium states, channel evolution, teleomatic change and least action principle, *Geomorphology*, 302, 3–19, <https://doi.org/10.1016/j.geomorph.2016.07.024>, <http://dx.doi.org/10.1016/j.geomorph.2016.07.024>, 2018.
- Napoli, E., Armenio, V., and De Marchis, M.: The effect of the slope of irregularly distributed roughness elements on turbulent wall-bounded flows, *Journal of Fluid Mechanics*, 613, 385–394, <https://doi.org/10.1017/S0022112008003571>, 2008.
- Nezu, I. and Nakagawa, H.: Turbulence in open-channel flows, *IAHR Monograph Series*, pp. 1–281, 1993.
- 580 Nield, J. M., King, J., Wiggs, G. F., Leyland, J., Bryant, R. G., Chiverrell, R. C., Darby, S. E., Eckardt, F. D., Thomas, D. S., Virca, L. H., and Washington, R.: Estimating aerodynamic roughness over complex surface terrain, *Journal of Geophysical Research Atmospheres*, 118, 12 948–12 961, <https://doi.org/10.1002/2013JD020632>, 2013.
- Nikora, V. I., Goring, D. G., and Biggs, B. J. F.: On gravel-bed roughness characterization, *Water Resources Research*, 34, 517–527, <https://doi.org/10.1029/97WR02886>, 1998.
- 585 Nikuradse, J.: *Laws of flow in rough pipes*, Tech. rep., Washington, D. C., 1933.
- Nowell, A. R. M. and Church, M. A.: Turbulent flow in a depth-limited boundary layer, *Journal of Geophysical Research*, 84, 4816–4824, <https://doi.org/10.1029/JC084iC08p04816>, 1979.
- Nyander, A.: *River-bed sediment surface characterisation using wavelet transform-based methods*, Doctoral thesis, Napier University, 2004.

- Nyander, A., Addison, P. S., McEwan, I., and Pender, G.: Analysis of river bed surface roughnesses using 2D wavelet transform-based methods, *Arabian Journal for Science and Engineering*, 28, 107–121, 2003.
- Parker, G. and Peterson, A. W.: Bar Resistance of Gravel-Bed Streams, *Journal of the Hydraulics Division*, 106, 1159–1575, 1980.
- Pelletier, J. D. and Field, J. P.: Predicting the roughness length of turbulent flows over landscapes with multi-scale microtopography, *Earth Surface Dynamics*, 4, 391–405, <https://doi.org/10.5194/esurf-4-391-2016>, 2016.
- Prestegard, K. L.: Bar resistance in gravel bed streams at bankfull stage, *Water Resources Research*, 19, 472–476, <https://doi.org/10.1029/WR019i002p00472>, 1983.
- Qin, J., Wu, T., and Zhong, D.: Spectral behavior of gravel dunes, *Geomorphology*, 231, 331–342, <https://doi.org/10.1016/j.geomorph.2014.12.023>, <http://dx.doi.org/10.1016/j.geomorph.2014.12.023>, 2015.
- Rickenmann, D. and Recking, A.: Evaluation of flow resistance in gravel-bed rivers through a large field data set, *Water Resources Research*, 47, <https://doi.org/10.1029/2010WR009793>, 2011.
- Robert, A.: Statistical properties of sediment bed profiles in alluvial channels, *Mathematical Geology*, 20, 205–225, <https://doi.org/10.1007/BF00890254>, 1988.
- Robert, A.: Fractal properties of simulated bed profiles in coarse-grained channels, *Mathematical Geology*, 23, 367–382, <https://doi.org/10.1007/BF02065788>, 1991.
- Schlichting, V. H.: Experimentelle untersuchungen zum Rauigkeitsproblem, *Archive of Applied Mechanics*, 7, 1–34, 1936.
- Schlichting, V. H.: *Boundary-Layer Theory*, McGraw-Hill, New York, 7th edn., 1979.
- Schultz, M. P. and Flack, K. A.: Turbulent boundary layers on a systematically varied rough wall, *Physics of Fluids*, 21, 1–9, <https://doi.org/10.1063/1.3059630>, 2009.
- Smart, G. M., Duncan, M. J., and Walsh, J. M.: Relatively Rough Flow Resistance Equations, *Journal of Hydraulic Engineering*, 128, 568–578, [https://doi.org/10.1061/\(ASCE\)0733-9429\(2002\)128:6\(568\)](https://doi.org/10.1061/(ASCE)0733-9429(2002)128:6(568)), 2002.
- Sundborg, A.: The River Klarälven: A Study of Fluvial Processes, *Geografiska Annaler*, 38, 125–237, 1956.
- Torrence, C. and Compo, G. P.: A practical guide to wavelet analysis, *Bulletin of the American Meteorological society*, 79, 61–78, 1998.
- Weichert, R. B., Bezzola, G. R., and Minor, H.-E.: Bed erosion in steep open channels, *Journal of Hydraulic Research*, 47, 360–371, <https://doi.org/10.3826/jhr.2009.3128>, 2009.
- Westoby, M. J., Brasington, J., Glasser, N. F., Hambrey, M. J., and Reynolds, J. M.: 'Structure-from-Motion' photogrammetry: A low-cost, effective tool for geoscience applications, *Geomorphology*, 179, 300–314, <https://doi.org/10.1016/j.geomorph.2012.08.021>, 2012.
- Wilcox, A. C. and Wohl, E. E.: Flow resistance dynamics in step-pool stream channels: 1. Large woody debris and controls on total resistance, *Water Resources Research*, 42, 1–16, <https://doi.org/10.1029/2005WR004277>, 2006.
- Wolman, M. G.: A method of sampling coarse river-bed material, *Transactions, American Geophysical Union*, 35, 951–956, 1954.
- Wolman, M. G. and Miller, J. P.: Magnitude and Frequency of Forces in Geomorphic Processes, *The Journal of Geology*, 68, 54–74, 1960.
- Yen, B. C.: Open channel flow resistance, *Journal of Hydraulic Engineering*, 128, 20–39, [https://doi.org/10.1061/\(ASCE\)0733-9429\(2002\)128:1\(20\)](https://doi.org/10.1061/(ASCE)0733-9429(2002)128:1(20)), 2002.
- Yochum, S. E., Bledsoe, B. P., Wohl, E. E., and David, G. C. L.: Spatial characterization of roughness elements in high-gradient channels of the Fraser Experimental Forest, Colorado, USA, *Water Resources Research*, 50, 6015–6029, <https://doi.org/10.1002/2014WR015587>, 2014.